Forecasting Crashes with a Smile

Ian Martin Ran Shi*

September, 2023

Abstract

We introduce a framework that uses option prices to deliver upper and lower bounds on the probability of crash in an individual stock, and argue based on a priori considerations that the lower bound should be close to the true crash probability. Empirical tests support this prediction in and out of sample. We horse-race the lower bound against a range of characteristics proposed by the prior literature. The lower bound is highly statistically significant, with a t-statistic above five, and is an order of magnitude more economically significant than any of the characteristics, in the sense that a one standard deviation increase in the lower bound raises the predicted probability of a crash by 3 percentage points, whereas a one standard deviation change in the next most important predictor (a measure of short interest) moves the predicted probability of a crash by only 0.3 percentage points.

*Martin: London School of Economics, i.w.martin@lse.ac.uk; Shi: University of Colorado Boulder, ran.shi@colorado.edu. We are grateful to Christopher Jones, Dasol Kim, Lukas Kremens, Scott Richardson, and to participants in seminars at LBS, LSE, the Office of Financial Research, and the 7th Annual Marshall PhD Conference in Finance for helpful comments.

In this paper, we propose a new way of estimating the probability of a crash in an individual stock. Our approach performs well in and out of sample, and outperforms a LASSO-based competitor that exploits characteristics that have been proposed as crash forecasters in the prior literature. As our forecasts are based solely on asset prices—namely, the prices of options on the stock in question, and of options on a broad stock index—they are, in principle, available in real time.

Aside from its intrinsic interest for investors and policymakers, forecasting crashes represents an interesting theoretical challenge for two reasons. First, there is an obvious and widely used competitor for our approach, the risk-neutral probability of a crash, which can be calculated from asset prices without any assumptions other than the absence of arbitrage. And yet it is natural to worry that the risk-neutral probabilities, which put more weight on bad states of the world, are likely to overstate the true probabilities of crashes.

Second, any attempt to forecast crashes in individual stocks using option prices seems to run into the problem that the inferred crash probability ought to reflect the correlation structure: the conclusions one would draw from a fixed set of prices should depend strongly on whether the stock in question has, for example, a positive or negative beta. But the prices of options on individual stocks and on the market reveal information only about the marginal risk-neutral distributions of those stocks and of the market, and not about the joint distribution.

We address these issues in two steps. To connect risk-neutral and true probabilities, we take the perspective of a myopic investor with power utility who chooses to invest his or her wealth fully in the S&P 500 index, which we treat as a proxy for "the market."[1] This implies that the stochastic discount factor (SDF) is proportional to a power of the return on the S&P 500 index. In the special case in which risk aversion equals zero, the predictive variable reduces to the risk-neutral probability of a crash, which can be inferred from out-of-the-money put option prices, following Breeden and Litzenberger (1978): this is a widely used indicator of crash probabilities but, as we will show, allowing for positive risk aversion improves predictive performance.

Evidently, the power utility assumption is restrictive. In an ideal world we would allow the SDF to depend on broader measures of wealth and potentially other state

[1] Related approaches have been adopted in the context of the stock market (Martin, 2017; Chabi-Yo and Loudis, 2020; Martin, 2021; Gao and Martin, 2021; Gandhi, Gormsen, and Lazarus, 2022), individual stocks (Martin and Wagner, 2019; Kadan and Tang, 2020; Chabi-Yo, Dim, and Vilkov, 2023), and currencies (Kremens and Martin, 2019; Della Corte, Gao, and Jeanneret, 2023).

variables. But option prices on the S&P 500 and on individual stocks are *observable*; and they are forward-looking. The great strength of our approach is that it allows us to avoid the alternative undesirable assumption, commonly made in the literature, that backward-looking historical measures are good proxies for the forward-looking measures that come out of theory. The empirical success of our approach suggests that the price of our assumption is worth paying.

Having made the assumption, it is straightforward to infer the true distribution of market returns from the risk-neutral distribution of market returns, as in Martin (2017). To calculate the true distribution of a given *stock's* returns, however, we would need to observe the *joint* risk-neutral distribution of that stock's and the market's returns. The problem is that observable option prices only allow us to infer the individual (that is, marginal) risk-neutral distributions of the stock and of the market, without giving us any control on the correlation structure.

This is the central challenge confronted by this paper. We handle it by exploiting the theory of copulas and, more specifically, the Fréchet–Hoeffding bounds. These allow us to derive upper and lower bounds on the true probabilities of a crash that apply (under our maintained assumption on the form of the SDF) for *any* correlation structure. As the bounds fully exploit information in the two marginal distributions, they are tighter than the naive bounds that follow from the fact that correlation must lie between plus and minus one.[2] (This paper might more accurately be titled "Forecasting Crashes with Two Smiles.")

We calculate bounds on the probability of declines of (at least) 5%, 10% or 20% over the next one, three, six, and twelve months, paying particular attention to the case of a 20% decline over one month, which corresponds most closely to the notion of a crash.

The bounds demonstrate significant variation across firms and over time. Figure 1 illustrates by plotting upper and lower bounds on the probability of a crash of at least 20% over a one-month horizon for Apple and AIG. Figure 2 plots the time-series of the cross-sectional median of the upper and lower bounds on crash probabilities, together with the probability of a crash in the market. The market crash probability tends to be lower and less volatile than the individual stock probabilities.

The lower bound is tight if a stock's return is a monotonic (and potentially nonlinear)

[2] Other than in the special case in which the market and individual stock returns are jointly lognormal. Fortunately, we will see that this is not the case in practice. Ours is, therefore, a relatively unusual setting in which nonlognormality is helpful rather than unhelpful.

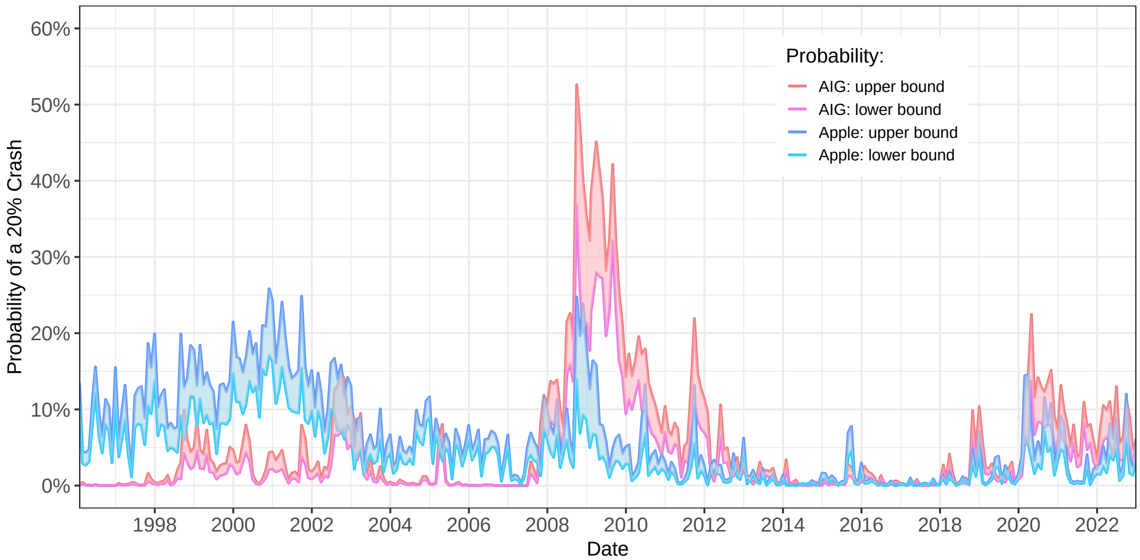

Figure 1: Bounds on forward-looking probabilities of a crash (one-month net return being less than -20%) for Apple and AIG.

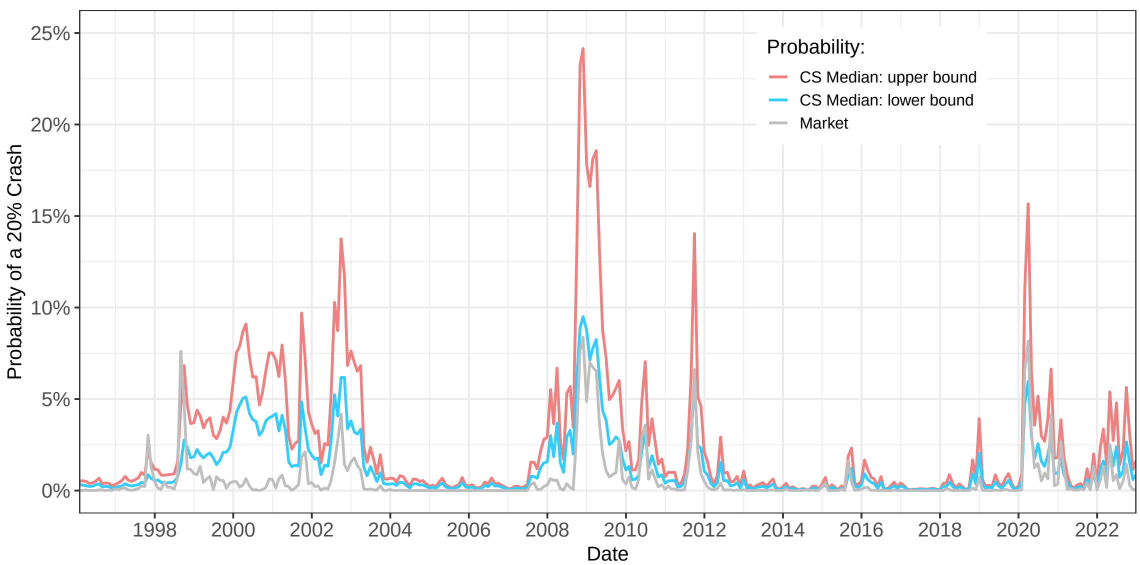

Figure 2: Time series of the cross-sectional medians of the upper and lower bounds on forward-looking probabilities of a crash (one-month net return being less than -20%); and of the crash probability of the S&P 500 index, based on the approach in Martin (2017).

increasing function of the market return, while the upper bound is tight if a stock's return is a monotonic decreasing function of the market return. A priori, the former case is more plausible, so we expect that, of the two bounds, the lower bound is a better measure of the true crash probability. To assess this prediction, we regress realized crash indicators onto the upper bound and onto the lower bound. We consider crashes of size 5%, 10%, and 20% over horizons of one, three, six, and 12 months, and find that both bounds are statistically significant predictors of crashes at all horizons and for all crash sizes. The same is true for the risk-neutral probability of a crash (which we show must always lie between the upper and lower bounds).

If the lower bound were a perfect measure of the crash probability, we would find an intercept equal to zero and slope coefficient equal to one in the associated regression. And indeed we do find, for all 12 horizon/crash-size pairs, intercepts that are not significantly different from zero and slope coefficients that are significantly positive and close to one. The lower bound also outperforms the risk-neutral probability in an R^2 sense for 11 of the 12 horizon/crash-size pairs (the single exception being the one-year/5% pair).

The lower bound remains significant when we include fifteen stock characteristics that the prior literature has found useful in accounting for stock return variation, forecasting crashes, or predicting bankruptcies: CAPM beta, firm size, the book-to-market ratio, gross profits divided by total assets, three measures of trailing returns, realized volatility of market-adjusted returns, turnover, one-year sales growth, short interest scaled by institutional ownership, leverage, net income to assets, cash to assets, and log price per share. At horizons of one month and one quarter, the lower bound on its own achieves a higher R^2 than all fifteen stock characteristics do together.

We also test the validity and tightness of our bounds for stock crash probabilities, following the approach of Back, Crotty, and Kazempour (2022). At all horizons and for all crash sizes, we do not reject the null that the bounds are valid (that is, the lower bounds are smaller and upper bounds are larger than the true crash probabilities). As expected, we strongly reject the hypothesis that the upper bound is tight (with p-values on the null hypothesis of tightness that never exceed 0.02 at any horizon or crash size), while the evidence is mixed on whether the lower bound is tight: we do not reject tightness at the one-month and one-year horizons, but at the three-month and six-month horizons we can reject tightness (with p-values between 0.02 and 0.06).

We conclude by comparing the out-of-sample predictive performance of the lower bound with the other stock characteristics. We split the dataset into a training and a testing sample and combine the stock characteristics via linear and logistic regressions, using a LASSO approach (Tibshirani, 1996) to select models through cross-validation in the training sample. The lower bound outperforms the resulting predictor at all horizons.

Related Literature. A large literature proposes methods to recover risk-neutral return densities from option prices. An incomplete list includes Breeden and Litzenberger (1978); Rubinstein (1994); Jackwerth and Rubinstein (1996); Aït-Sahalia and Lo (1998); Carr and Madan (2001). Christoffersen, Jacobs, and Chang (2013) provide a survey. While the starting point of our derivation relies on the insights of Breeden and Litzenberger (1978), the major challenge of bounding the physical, as oppose to risk-neutral, expectations is addressed by the new approach introduced in this paper.

Our work builds on a variety of papers that have studied the predictability of crashes. Bates (1991) presents evidence that put option prices helped to forecast the stock market crash of 1987. Chen, Hong, and Stein (2001) show that characteristics such as turnover and past returns forecast negative return skewness in individual stocks. Greenwood, Shleifer, and You (2019) use characteristics to forecast crashes at the industry level conditional on observing past price surge. Daniel, Klos, and Rottke (2023) document that price run-ups combined with high short interest and low institutional ownership forecast lower stock returns. Goetzmann, Kim, and Shiller (2022) find that "crash narratives" forecast future VIX levels, though not future market returns. There is also a literature that focuses on how measures of downside, skewness, and tail-risk are priced in the cross section of stock returns (see, for example, Ang, Chen, and Xing (2006); Boyer, Mitton, and Vorkink (2009); Vilkov and Xiao (2013); Kelly and Jiang (2014); Pederzoli (2021)).

The rest of this paper is organized as follows. Section 1 introduces our methodological approach and establishes various theoretical properties of the bounds. Section 2 provides details of our data sample. Section 3 presents our empirical results. Section 4 generalizes the approach. Section 5 concludes. All proofs are in the Appendix.

1 Theory

We adopt the perspective of an investor ("the investor") with power utility over next-period wealth who is marginal in all markets, including option markets, but who chooses to invest her wealth fully in the market, by which we mean the S&P 500 index. At time t, the investor chooses portfolio weights $\boldsymbol{w} = [w_1, \ldots, w_n]^\top$ to solve the problem[3]

$$\underset{\boldsymbol{w}}{\text{maximize}} \quad \mathbb{E}\left[u\left(\boldsymbol{w}^\top \boldsymbol{R}\right)\right] \quad \text{s.t.} \ \sum_{i=1}^{n} w_i = 1,$$

where $u(x) = x^{1-\gamma}/(1-\gamma)$, risk aversion equals γ, and we write $\boldsymbol{R} = [R_1, \ldots, R_n]^\top$ for the vector of gross returns on the n assets from time t to time $t+1$. The first-order conditions for this problem are

$$\mathbb{E}\left[\left(\boldsymbol{w}^\top \boldsymbol{R}\right)^{-\gamma} R_i\right] = \lambda \quad \text{for all } i,$$

where λ is a Lagrange multiplier. By assumption, the investor chooses to invest fully in the market, thus the market return, R_m, satisfies $R_m = \boldsymbol{w}^\top \boldsymbol{R}$. It follows that $M = R_m^{-\gamma}/\lambda$ is a stochastic discount factor (SDF).

For any tradable payoff X, the risk-neutral expectation of X (which we denote with an asterisk) satisfies, by definition,

$$\frac{1}{R_f}\mathbb{E}^*[X] = \mathbb{E}[MX]$$

where R_f is the gross risk-free rate: the two sides of the above equation represent different notational conventions for expressing the price at time t of a claim to the payoff X paid at time $t+1$. As $M\lambda R_m^\gamma \equiv 1$, it follows that

$$\mathbb{E}[X] = \mathbb{E}[M\lambda R_m^\gamma X] = \lambda \mathbb{E}[M(R_m^\gamma X)] = \frac{\lambda}{R_f}\mathbb{E}^*[R_m^\gamma X]\,. \tag{1}$$

Setting $X = 1$ in this equation, we must have $R_f = \lambda \mathbb{E}^*[R_m^\gamma]$; using this fact to eliminate λ from equation (1), we have

$$\mathbb{E}[X] = \frac{\mathbb{E}^*[R_m^\gamma X]}{\mathbb{E}^*[R_m^\gamma]}. \tag{2}$$

Hence we can infer the investor's expectation of X if we can *price* a claim to $R_m^\gamma X$.

For the rest of the paper we will assume that the payoff $X = h(R_i)$ is a well-behaved function of the return on a particular asset i, where $h : \mathbb{R}_+ \mapsto \mathbb{R}$ is continuous almost everywhere. We will denote by Q_{mi} the joint risk-neutral cumulative distribution function (CDF) of the market and individual stock return (R_m, R_i), and by Q_m and Q_i the corre-

[3] All expectations are conditional on current, time t, information. We suppress time subscripts to streamline the notation.

sponding marginal CDFs of R_m and R_i individually. Equation (2) can then be rewritten

$$\mathbb{E}[h(R_i)] = \frac{\int x^\gamma h(y)\, \mathrm{d}Q_{mi}(x, y)}{\int x^\gamma \, \mathrm{d}Q_m(x)}. \tag{3}$$

For example, if $X = \boldsymbol{I}(R_i \leq q)$ is the indicator function for the event that stock i's gross return is less than q, then equation (2) implies that

$$\mathbb{P}[R_i \leq q] = \frac{\mathbb{E}^*[R_m^\gamma \boldsymbol{I}(R_i \leq q)]}{\mathbb{E}^*[R_m^\gamma]}, \tag{4}$$

because $\mathbb{P}[R_i \leq q] = \mathbb{E}[\boldsymbol{I}(R_i \leq q)]$. Equation (4) shows that we can in principle infer the true probability distribution of a particular stock return, as perceived by the power utility investor who is holding the market, from risk-neutral distributions.

The challenge, however, is that while index options and individual stock options reveal risk-neutral expectations of *univariate* functions of index or stock returns, they do not reveal risk-neutral expectations of two- (or higher-) dimensional functions of index *and* stock returns simultaneously, as would be needed to calculate the numerators in (3) or (4).[4] Options on the market and on large-cap individual stocks are liquid, but because they are written on a single underlying asset they reveal only the marginal risk-neutral distributions, and not the correlation structure. To recover the risk-neutral joint distribution, one would need to observe the prices of derivatives whose payoffs are functions both of the stock index *and* of the stock of interest. But such prices are not observable in practice. (By contrast the probability of a crash in the market itself, as plotted in Figure 2, is relatively easy to handle: when $i = m$ the right-hand side of (4) is a ratio of risk-neutral expectations of functions of the single random variable R_m, which can be calculated from index option prices in the usual way.)

We can, nonetheless, derive bounds on the right-hand sides of (3) or (4). To do so, it is convenient to decompose the joint distribution into two parts: the marginals and the dependence structure. The marginals can be inferred from index and stock options, using the Breeden–Litzenberger approach. Roughly speaking, we can then bound the integral in the numerator of (3) by minimizing and maximizing over all possible dependence structures—more precisely, over all *copulas*.

[4] Ross (1976) showed in a finite-state setting that options on portfolios of assets could in principle be used to recover risk-neutral joint densities. Martin (2018) points out that this result fails with continuous states, and even with finite states given the assets that are traded in practice.

Definition 1. *A (two-dimensional) copula is a function* $C : [0,1]^2 \mapsto [0,1]$ *with the following properties:*

1. *C is grounded: $C(x,0) = C(0,y) = 0$ for any (x,y) in its domain;*
2. *$C(x,1) = x$ and $C(1,y) = y$ for any (x,y) in its domain;*
3. *C is two-increasing: for all rectangles $B = [x_1, y_1] \times [x_2, y_2] \subset [0,1]^2$, the "volume" of B, which is defined by $V_H(B) = C(x_2, y_2) - C(x_2, y_1) - C(x_1, y_2) + C(x_1, y_1)$ is non-negative.*

The following theorem of Sklar (1959) shows that any joint distribution can be associated with a copula that "glues together" its two marginals.

Theorem 1 (Sklar)**.** *Let Q be the joint CDF for the random vector (X, Y) with marginal CDFs F_X and F_Y. Then there exists a copula C, such that for all $x, y \in \mathbb{R}$,*

$$Q(x,y) = C(F_X(x),\, F_Y(y)).$$

We can therefore express the joint risk-neutral distribution of the market and stock return as $Q_{mi}(x,y) = C(Q_m(x), Q_i(y))$, where the risk-neutral index and individual stock CDFs, Q_m and Q_i, can be calculated from index and individual stock option prices. Although $C(\cdot,\cdot)$ is unknown, the following theorem supplies pointwise bounds that apply to any copula.

Theorem 2 (Fréchet–Hoeffding)**.** *If $C(u,v)$ is a copula, then*

$$\max(u+v-1, 0) \le C(u,v) \le \min(u,v), \quad (u,v) \in [0,1]^2.$$

Using this theorem, together with work of Tchen (1980), we have the following result, whose proof is in the Appendix.

Result 1. *For a continuous and two-increasing*[5] *function g defined on $[0,\infty) \times [0,\infty)$, we have the bounds*

$$\mathbb{E}^*\left[g\left(R_m,\, Q_i^{-1}\left(1 - Q_m(R_m)\right)\right)\right] \le \mathbb{E}^*[g(R_m,\, R_i)] \le \mathbb{E}^*\left[g\left(R_m,\, Q_i^{-1}\left(Q_m(R_m)\right)\right)\right]. \quad (5)$$

Result 1 provides bounds on the price of an asset whose payoff $g(R_m, R_i)$ can depend in an arbitrary way on the correlation structure of R_m and R_i. As the one-dimensional

[5] See Definition 1.

risk-neutral distributions are observable from index and individual stock option prices, we can treat Q_i and Q_m as *observable functions*. Thus the upper and lower bounds in (5) are risk-neutral expectations of known functions of the *single* variable R_m. They can therefore be calculated given observable index option prices.

Result 1 exhibits bounds that relate risk-neutral expectations of different random variables to one another. It does not rely on any assumptions about the form of the SDF. But, under our assumption on the power utility form of the SDF, we can set $g(x,y) = x^\gamma h(y)$, as in equation (3), to derive the following result.

Result 2. *Let h be a continuous increasing function defined on $[0,\infty)$ that does not cross the x-axis (that is, $h(x)h(y) \geq 0$ for any $x, y \geq 0$), and suppose the SDF is proportional to $R_m^{-\gamma}$. Then*

$$\frac{\mathbb{E}^*\left[R_m^\gamma h\left(Q_i^{-1}\left(1-Q_m(R_m)\right)\right)\right]}{\mathbb{E}^*\left[R_m^\gamma\right]} \leq \mathbb{E}[h(R_i)] \leq \frac{\mathbb{E}^*\left[R_m^\gamma h\left(Q_i^{-1}\left(Q_m(R_m)\right)\right)\right]}{\mathbb{E}^*\left[R_m^\gamma\right]}.$$

These bounds are sharp, in the sense that the lower bound is achieved if the return on the stock and return on the market are countermonotonic, and the upper bound is achieved if the return on the stock and return on the market are comonotonic.[6]

Note that the middle expectation above is a true—not a risk-neutral—expectation. In our application to crash probabilities, we set $h(x) = -\boldsymbol{I}(x \leq q)$ in Result 2. This delivers the following special case of Result 2 on which our empirical work is based.

Result 3. *The probability of a crash in stock i, $\mathbb{P}[R_i \leq q]$, satisfies the bounds*

$$\frac{\mathbb{E}^*\left[R_m^\gamma \boldsymbol{I}\left(R_m \leq q_l\right)\right]}{\mathbb{E}^*\left[R_m^\gamma\right]} \leq \mathbb{P}\left[R_i \leq q\right] \leq \frac{\mathbb{E}^*\left[R_m^\gamma \boldsymbol{I}\left(R_m \geq q_u\right)\right]}{\mathbb{E}^*\left[R_m^\gamma\right]},$$

where $q_l = Q_m^{-1}(Q_i(q))$ and $q_u = Q_m^{-1}(1-Q_i(q))$.

The lower bound is attained if the return on the stock and return on the market are comonotonic. The upper bound is attained if the two returns are countermonotonic.

The risk-neutral probability of a crash, $\mathbb{P}^*[R_i \leq q]$, lies between the two bounds.

As most stocks typically move with, rather than against, the market, we anticipate that comonotonicity is closer to the truth than countermonotonicity. Hence, a priori,

[6] Two random variables are said to be countermonotonic if one is a monotonically decreasing transformation of the other, and comonotonic if one is a monotonically increasing transformation of the other.

we expect the lower bound to be tighter—closer to the true crash probability—than the upper bound. Our empirical results in Section 3.1 support this intuition, showing that the lower bounds do indeed track the forward-looking crash probabilities better in the panel of S&P 500 stocks.

Our next result shows that the bounds widen as risk aversion rises.

Result 4. *The lower bound is decreasing in γ and the upper bound is increasing in γ.*

When $\gamma = 0$, the lower and the upper bounds are both equal to $\mathbb{P}^*[R_i \leq q]$: this is the case in which the true and risk-neutral expectations coincide, so that crash probabilities can be inferred perfectly from option prices.

As $\gamma \to \infty$, the bounds become trivial: for any q such that $0 < Q_i(q) < 1$, the lower bound tends to 0 and the upper bound tends to 1.

It follows that higher risk aversion leads to more conservative bounds: increasing risk aversion drives the lower bound down and the upper bound up.

It only remains to show how we calculate the bounds that appear in Result 3. Given a chosen value of q, and hence of q_l and q_u, the risk-neutral expectations that appear in the bounds can be calculated from index option prices. The only point at which the prices of options *on stock i itself* are used is, therefore, in the calculation of q_l and q_u, which are determined by the prices of index and of individual stock options via the risk-neutral marginals $Q_m(\cdot)$ and $Q_i(\cdot)$.

Result 5. *For any $\gamma > 0$, we can calculate the risk-neutral expectations in Result 3 using observable option prices:*

$$\mathbb{E}^*\left[R_m^\gamma\right] = R_f^\gamma + \frac{R_f}{S_0^\gamma}\left[\int_0^F \gamma(\gamma-1)K^{\gamma-2}\mathrm{put}(K)\,\mathrm{d}K + \int_F^\infty \gamma(\gamma-1)K^{\gamma-2}\mathrm{call}(K)\,\mathrm{d}K\right]$$

$$\mathbb{E}^*\left[R_m^\gamma \boldsymbol{I}\left(R_m \leq q_l\right)\right] = R_f q_l^\gamma\left[\mathrm{put}'(K_l) - \gamma\frac{\mathrm{put}\left(K_l\right)}{K_l}\right] + \frac{R_f}{S_0^\gamma}\int_0^{K_l}\gamma(\gamma-1)K^{\gamma-2}\mathrm{put}\left(K\right)\,\mathrm{d}K$$

$$\mathbb{E}^*\left[R_m^\gamma \boldsymbol{I}\left(R_m \geq q_u\right)\right] = R_f q_u^\gamma\left[\gamma\frac{\mathrm{call}(K_u)}{K_u} - \mathrm{call}'(K_u)\right] + \frac{R_f}{S_0^\gamma}\int_{K_u}^\infty\gamma(\gamma-1)K^{\gamma-2}\mathrm{call}\left(K\right)\,\mathrm{d}K$$

where S_0 is the spot price of the market index; $F = R_f S_0$ is the forward price; $\mathrm{put}(K)$ *and* $\mathrm{call}(K)$ *are the prices of index put and call options; and $K_l = q_l S_0$ and $K_u = q_u S_0$.*

1.1 Fréchet–Hoeffding vs. Cauchy–Schwarz

The bounds in Result 3 are stronger than the bounds that follow from the fact that correlation lies between plus and minus one (that is, from the Cauchy–Schwarz inequality). To compare the two approaches, rewrite equation (4) as

$$\mathbb{P}\left[R_i \leq q\right] = \mathbb{P}^*\left[R_i \leq q\right] + \frac{\operatorname{cov}^*\left[R_m^\gamma, \boldsymbol{I}(R_i \leq q)\right]}{\mathbb{E}^*\left[R_m^\gamma\right]}.$$

As correlation must lie between plus and minus one, it follows that

$$\mathbb{P}^*\left[R_i \leq q\right] - \frac{\sigma^*\left[R_m^\gamma\right]\sigma^*\left[\boldsymbol{I}(R_i \leq q)\right]}{\mathbb{E}^*\left[R_m^\gamma\right]} \leq \mathbb{P}\left[R_i \leq q\right] \leq \mathbb{P}^*\left[R_i \leq q\right] + \frac{\sigma^*\left[R_m^\gamma\right]\sigma^*\left[\boldsymbol{I}(R_i \leq q)\right]}{\mathbb{E}^*\left[R_m^\gamma\right]}, \tag{6}$$

where $\sigma^*[\cdot] = \sqrt{\operatorname{var}^*[\cdot]}$ denotes risk-neutral volatility. These bounds depend only on univariate risk-neutral expectations, so can be calculated from observable option prices.

But this approach is less efficient than the bounds derived above, because comonotonic random variables are in general not perfectly positively correlated, and countermonotonic random variables are in general not perfectly negatively correlated.[7] It follows that bounds obtained by "setting correlation equal to one" (or to minus one) will in general be looser than the bounds supplied by Result 3.

Table A2, in the appendix, demonstrates the advantages of our approach by reporting the relative widths of our bounds compared with the Cauchy–Schwarz bounds across firms. The bounds based on the Fréchet–Hoeffding theorem are between 23% and 71% narrower than the Cauchy–Schwarz bounds, with the best relative performance occurring for the 1 month/20% pair which most closely conforms to the notion of a crash.

2 Data

We focus on firms included in the S&P 500 index, using index constituent information from Compustat. Our sample runs from January 1996 to December 2022. On the last trading day of each month t, we obtain, from OptionMetrics, the volatility surfaces of the S&P 500 index and of all firms that are S&P 500 constituents during month t, together with risk-free rates. We then obtain stock prices, returns, trading volumes and shares

[7] As a simple example, if Z is Normal then e^Z and $e^{\sigma Z}$ are lognormal; they are comonotonic if $\sigma > 0$ and countermonotonic if $\sigma < 0$. But as σ tends to plus or minus infinity, the correlation between the two random variables tends to zero, as is easily checked via a straightforward calculation.

outstanding from CRSP to construct a firm-month panel.

We face the issue that individual stock options are American style rather than European style. We deal with this issue, following the related literature (Carr and Wu, 2009; Kelly, Lustig, and Van Nieuwerburgh, 2016; Christoffersen, Fournier, and Jacobs, 2018; Martin and Wagner, 2019), by using volatility surfaces reported by OptionMetrics, who use proprietary multinomial tree models to account for early exercise premia. In any case, we believe that the distinction is likely to be relatively minor for our applications, as the calculations required by Results 3 and 5 depend on the prices of out-of-the-money options.

When calculating the integrals in Result 5, we extrapolate a flat volatility smile outside the range of observed strikes, as is also standard in the literature. Additional computational details for constructing our bounds are relegated to Section B of the Appendix.

3 Empirical Results

We write $R_{i,t\to t+\tau}$ for the gross return on stock i from time t to time $t+\tau$, $\mathbb{P}^L_{i,t}(\tau,q)$ and $\mathbb{P}^U_{i,t}(\tau,q)$ for the lower and upper bounds on the probability that $R_{i,t\to t+\tau}$ is less than or equal to q, and $\mathbb{P}^*_{i,t}(\tau,q)$ for the corresponding risk-neutral probability. We set risk aversion, γ, to two throughout.

Table 1 reports summary statistics for these measures with $q = 80\%$, 90% and 95%, at 1, 3, 6, and 12 month horizons. For comparison, we also report the realized frequencies of crashes. Specifically, for each month from January 1996 to December 2022, we calculate cross-sectional averages of the realized crash indicator $\boldsymbol{I}(R_{i,t\to t+\tau} \leq q)$ (which equals one if the realized return is less than or equal to q, and zero otherwise), the upper and lower bounds, and the risk-neutral crash probabilities. The first four columns of the table report the means and standard deviations of these $T = 324$ observations at each of the four horizons.

Similarly, we calculate time-series averages of the same quantities for each of the $N = 1044$ firms in our sample. The last four columns of Table 1 report the means and standard deviations of these time-series averages. The sample means of cross-sectional and time-series averages differ slightly because we have an unbalanced panel.

Consistent with the predictions of the theory and the discussion following Result 3, the time-series and cross-sectional means of the lower bounds are close to the corresponding mean realized crash frequencies, whereas the risk-neutral probabilities and (even more so) the upper bounds overestimate the likelihood of crashes.

Table 1: Summary statistics

This table presents summary statistics of realized crash events, our crash probability bounds, and risk-neutral crash probabilities. The sample data are monthly from January 1996 to December 2022. The crash events (realized crashes) under consideration are $\boldsymbol{I}(R_{i,t\to t+\tau} \leq q)$ for $q = 0.80$, 0.90, 0.95 and $\tau =$ 1, 3, 6, 12 months. The bounds and risk-neutral probabilities are measures of the conditional probabilities of crash events.

		averaged across firms (number of obs. $T = 324$)				averaged across time (number of obs. $N = 1044$)			
	horizon	1	3	6	12	1	3	6	12
Panel A: $q = 0.80$, down by over 20%									
realized	mean	0.021	0.069	0.111	0.152	0.029	0.084	0.130	0.173
	s.d.	0.048	0.107	0.141	0.160	0.059	0.092	0.129	0.166
lower bound	mean	0.022	0.073	0.102	0.123	0.027	0.079	0.110	0.133
	s.d.	0.020	0.029	0.028	0.027	0.029	0.046	0.052	0.056
upper bound	mean	0.038	0.144	0.233	0.339	0.044	0.152	0.242	0.350
	s.d.	0.040	0.071	0.082	0.098	0.042	0.069	0.079	0.089
risk-neutral	mean	0.031	0.113	0.173	0.236	0.037	0.120	0.181	0.245
	s.d.	0.031	0.050	0.053	0.059	0.036	0.058	0.065	0.072
Panel B: $q = 0.90$, down by over 10%									
realized	mean	0.096	0.173	0.211	0.236	0.110	0.191	0.231	0.252
	s.d.	0.124	0.170	0.185	0.196	0.089	0.119	0.152	0.183
lower bound	mean	0.109	0.168	0.196	0.210	0.118	0.179	0.206	0.219
	s.d.	0.037	0.031	0.028	0.023	0.050	0.055	0.056	0.056
upper bound	mean	0.156	0.277	0.366	0.466	0.166	0.289	0.378	0.475
	s.d.	0.064	0.074	0.081	0.087	0.062	0.070	0.074	0.074
risk-neutral	mean	0.136	0.228	0.286	0.341	0.145	0.239	0.297	0.350
	s.d.	0.051	0.051	0.051	0.050	0.056	0.061	0.063	0.063
Panel C: $q = 0.95$, down by over 5%									
realized	mean	0.216	0.271	0.288	0.289	0.230	0.287	0.306	0.306
	s.d.	0.187	0.200	0.204	0.210	0.101	0.122	0.155	0.185
lower bound	mean	0.215	0.264	0.277	0.271	0.228	0.275	0.286	0.279
	s.d.	0.036	0.024	0.020	0.020	0.052	0.049	0.047	0.048
upper bound	mean	0.281	0.393	0.465	0.541	0.294	0.404	0.474	0.548
	s.d.	0.064	0.064	0.066	0.074	0.059	0.058	0.056	0.057
risk-neutral	mean	0.251	0.332	0.375	0.408	0.264	0.343	0.383	0.415
	s.d.	0.049	0.041	0.038	0.040	0.055	0.052	0.049	0.050

3.1 In-sample tests

3.1.1 Regression tests

To test whether the option-implied bounds successfully measure the probability of a crash, we run the regression

$$\boldsymbol{I}(R_{i,t\to t+\tau} \le q) = \alpha + \beta X_{i,t}(\tau, q) + \varepsilon_{i,t+\tau} \tag{7}$$

for a range of crash sizes q and forecasting horizons τ. Here $X_{i,t}(\tau, q)$ is the lower or upper bound on the crash probability (that is, $\mathbb{P}^L_{i,t}(\tau, q)$ or $\mathbb{P}^U_{i,t}(\tau, q)$), or the risk-neutral crash probability, $\mathbb{P}^*_{i,t}(\tau, q)$. Result 3 showed, under our maintained assumptions, that the inequality

$$\mathbb{P}^L_{i,t}(\tau, q) \le \mathbb{P}_t[R_{i,t\to t+\tau} \le q] \le \mathbb{P}^U_{i,t}(\tau, q)$$

holds for any stock i, forecasting horizon τ, and crash size q. If, moreover, one of the bounds is close to the true crash probability, we should find α close to zero and β close to one in the corresponding regression.

The regression results are shown in Table 2, which reports two-way clustered standard errors in parentheses, following Thompson (2011), and block bootstrapped standard errors in square brackets, using the procedure of Martin and Wagner (2019). Across crash sizes and forecasting horizons—and for all three right-hand side variables—the estimated intercepts are close to zero, while the estimated slope coefficients are positive and strongly significant.

The estimated slope coefficients exhibit a clear monotonic pattern[8] that is consistent with the theory. The estimated coefficients on the lower bound are largest (averaging around 1.03 across crash sizes and horizons); the estimated coefficients on the risk-neutral probability are significantly below one (averaging around 0.75); and the estimated coefficients on the upper bound are smallest (averaging around 0.53).

In the case of the lower bound, the estimated coefficients are insignificantly different from one at all horizons and for all crash sizes. Again, this is consistent with the discussion following Result 3. The lower bound also outperforms the other two variables in an R^2 sense for almost all horizons and crash sizes.

Tables A3, A4 and A5, in the appendix, report the same regressions with time fixed

[8] Recall from Result 3 that the risk-neutral probability must lie between the upper and lower bounds.

Table 2: Regression tests of the option-implied crash probability bounds

This table reports the results from regressing the indicator function of realized equity returns being less than a threshold q on the option-implied physical probability bounds, $\mathbb{P}^L_{i,t}(\tau, q)$ and $\mathbb{P}^U_{i,t}(\tau, q)$, as well as the risk-neutral probabilities $\mathbb{P}^*_{i,t}(\tau, q)$. The data are monthly from January 1996 to December 2022. Firms under consideration are S&P 500 constituents. The return horizon τ is one month, three months, six months, or one year. Results in Panels A, B, and C are from the linear regressions,

$$\boldsymbol{I}(R_{i,t\to t+\tau} \le q) = \alpha + \beta X_{it}(\tau, q) + \varepsilon_{i,t+\tau},$$

in which $q = 0.80, 0.90$ and 0.95, and X stands for $\mathbb{P}^L$ (the lower bounds), $\mathbb{P}^U$ (the upper bounds), or $\mathbb{P}^*$ (the risk-neutral probabilities). The values in parentheses are firm-month two-way clustered standard errors following Thompson (2011). The values in square brackets are standard errors following the panel bootstrap procedures of Martin and Wagner (2019) using 2500 bootstrap samples.

	lower bound				upper bound				risk neutral			
horizon	1	3	6	12	1	3	6	12	1	3	6	12
	Panel A: $q = 0.80$, down by over 20%											
α	0.00	−0.01	−0.01	0.02	0.00	0.00	0.00	0.01	0.00	−0.01	−0.02	0.00
	(0.00)	(0.01)	(0.01)	(0.01)	(0.00)	(0.01)	(0.01)	(0.02)	(0.00)	(0.01)	(0.01)	(0.02)
	[0.00]	[0.01]	[0.01]	[0.01]	[0.00]	[0.01]	[0.02]	[0.03]	[0.00]	[0.01]	[0.01]	[0.03]
β	0.92	1.03	1.15	1.08	0.55	0.51	0.50	0.41	0.68	0.69	0.73	0.66
	(0.11)	(0.09)	(0.09)	(0.08)	(0.08)	(0.06)	(0.06)	(0.06)	(0.09)	(0.07)	(0.07)	(0.08)
	[0.11]	[0.15]	[0.14]	[0.12]	[0.08]	[0.08]	[0.09]	[0.10]	[0.08]	[0.10]	[0.12]	[0.13]
R^2	5.66%	5.17%	4.78%	3.76%	5.29%	4.13%	3.26%	2.33%	5.45%	4.51%	3.91%	3.00%
	Panel B: $q = 0.90$, down by over 10%											
α	−0.02	−0.01	−0.01	0.02	−0.02	0.00	0.01	0.05	−0.02	−0.02	−0.02	0.00
	(0.01)	(0.01)	(0.01)	(0.02)	(0.01)	(0.02)	(0.02)	(0.04)	(0.01)	(0.02)	(0.02)	(0.03)
	[0.01]	[0.01]	[0.02]	[0.03]	[0.01]	[0.03]	[0.03]	[0.06]	[0.01]	[0.02]	[0.03]	[0.04]
β	1.05	1.07	1.12	1.03	0.75	0.63	0.54	0.41	0.88	0.83	0.81	0.69
	(0.08)	(0.07)	(0.07)	(0.08)	(0.07)	(0.07)	(0.07)	(0.08)	(0.08)	(0.08)	(0.08)	(0.09)
	[0.08]	[0.10]	[0.11]	[0.13]	[0.07]	[0.11]	[0.10]	[0.13]	[0.08]	[0.11]	[0.12]	[0.14]
R^2	5.47%	3.73%	3.43%	2.54%	5.36%	3.06%	2.20%	1.25%	5.47%	3.41%	2.84%	1.88%
	Panel C: $q = 0.95$, down by over 5%											
α	0.00	0.02	−0.01	0.05	0.00	0.05	0.06	0.11	0.00	0.01	−0.01	0.04
	(0.01)	(0.02)	(0.02)	(0.03)	(0.02)	(0.03)	(0.04)	(0.05)	(0.02)	(0.03)	(0.03)	(0.05)
	[0.01]	[0.03]	[0.03]	[0.06]	[0.02]	[0.05]	[0.06]	[0.09]	[0.02]	[0.04]	[0.05]	[0.07]
β	0.98	0.95	1.06	0.88	0.76	0.56	0.49	0.33	0.88	0.77	0.80	0.61
	(0.07)	(0.07)	(0.08)	(0.10)	(0.08)	(0.09)	(0.09)	(0.10)	(0.08)	(0.09)	(0.10)	(0.12)
	[0.06]	[0.10]	[0.11]	[0.18]	[0.08]	[0.13]	[0.14]	[0.17]	[0.08]	[0.12]	[0.14]	[0.17]
R^2	3.01%	1.85%	1.86%	1.36%	3.02%	1.35%	0.94%	0.49%	3.08%	1.64%	1.45%	0.93%

effects, firm fixed effects, and time *and* firm fixed effects, respectively. (Although such specifications are not useful for prediction without prior knowledge of the values of the fixed effects, they help us to understand where the success of the predictor variables comes from.) Table A3 shows that the slope coefficients are little changed by the introduction of time fixed effects: thus our measures successfully explain cross-sectional variation in crash probabilities. Tables A4 and A5 show that the slope coefficients remain highly significant at short horizons when firm fixed effects are included, either on their own or even jointly with time fixed effects (but not at the 12 month horizon, or at the 6 month horizon for the smallest "crash" size, $q = 0.95$). For example, at the one-month horizon with both time and firm fixed effects included, the coefficient on the lower bound is 0.73 for the largest crashes ($q = 0.8$), 0.65 for intermediate crashes ($q = 0.90$), and 0.43 for the smallest crashes ($q = 0.95$), with standard errors in the range 0.04 to 0.10.

3.1.2 Validity and tightness tests

We now carry out formal tests of the validity and tightness of the crash probability bounds based on conditional moment restrictions, following Back, Crotty, and Kazempour (2022) (henceforth, BCK).

Let $\boldsymbol{z}_t$ be a strictly positive vector of dimension d that incorporates conditioning variables known at time t. This vector includes a set of candidate variables that might help to determine crash probabilities, and it determines another vector, of the same length,

$$\lambda = \mathbb{E}\left[\left\{\boldsymbol{I}(R_{i,t\to t+\tau} \leq q) - X_{i,t}(\tau, q)\right\} \boldsymbol{z}_t\right],$$

where X represents lower or upper bounds. As each element of $\boldsymbol{z}_t$ is strictly positive, we can assess the validity of the lower bound[9] by testing $\lambda \geq 0$ against the alternative that $\lambda \in \mathbb{R}^d$ (that is, λ is unrestricted). If the lower bound is valid, we can assess its *tightness* by testing $\lambda = 0$ against the alternative $\lambda \geq 0$. Similarly, we can assess the validity of the upper bound by testing $\lambda \leq 0$ against the alternative $\lambda \in \mathbb{R}^d$, and assess its tightness by testing $\lambda = 0$ against the alternative $\lambda \leq 0$.

Following BCK, we include a constant in the vector $\boldsymbol{z}_t$, together with additional variables from Welch and Goyal (2008), transformed where necessary to guarantee positivity.

[9]If the lower bound is valid then $\mathbb{E}_t\left[\boldsymbol{I}(R_{i,t\to t+\tau} \leq q) - X_{i,t}(\tau, q)\right] \geq 0$, where $X_{i,t}(\tau, q) = \mathbb{P}^L_{i,t}(\tau, q)$. As $\boldsymbol{z}_t$ is known at time t and strictly positive, it follows that $\mathbb{E}_t\left[\left\{\boldsymbol{I}(R_{i,t\to t+\tau} \leq q) - X_{i,t}(\tau, q)\right\} \boldsymbol{z}_t\right] \geq 0$, and hence that $\mathbb{E}\left[\left\{\boldsymbol{I}(R_{i,t\to t+\tau} \leq q) - X_{i,t}(\tau, q)\right\} \boldsymbol{z}_t\right] \geq 0$ by the law of iterated expectations.

We then construct the estimator

$$\hat{\lambda} = \frac{1}{T} \sum_{t=1}^{T} \left[\frac{1}{N_t} \sum_{i=1}^{N_t} \left\{ \boldsymbol{I}(R_{i,t\to t+\tau} \leq q) - X_{i,t}(\tau, q) \right\} \boldsymbol{z}_t \right],$$

where N_t is the number of firms at time t, and estimate the variance-covariance matrix of $\hat{\lambda}$ using the Driscoll and Kraay (1998) estimator to account for heteroskedasticity and serial correlation in the time series and cross sectional dependence across firms.

Table 3 reports the results of the BCK tests. The headline result is that we do not reject validity of either the upper or lower bounds at any horizon or crash size.

For all horizons and crash sizes we can, however, strongly reject the hypothesis that the upper bound is tight. This is as expected: the upper bound is tight only if stock returns and the market return are countermonotonic—that is, if all individual stock returns are monotonically decreasing functions of the market return. This is implausible, even as an approximation, for a single stock; and it *cannot* hold for all stocks given that the market return is a weighted average of individual stock returns.

By contrast, and as noted above, we expect a priori that the lower bound should be closer to the truth. Here the evidence of tightness is more mixed. We do not reject tightness of the lower bound for any crash size at the 1-month horizon (with p-values on the null varying between 0.133 and 0.352) or 12-month horizon (p-values between 0.096 and 0.164); but we can reject tightness with moderate confidence at the 3-month horizon (p-values between 0.022 and 0.059) and 6-month horizon (p-values between 0.043 and 0.057).

3.1.3 Comparison with other predictor variables

For the rest of the paper, we focus on declines of at least 20%, which correspond most closely to the idea of a crash.

The previous section established that the theoretically motivated quantity $\mathbb{P}^L_{i,t}(\tau, q)$ is a strongly statistically significant univariate forecaster of crashes, and that it is a valid lower bound on the probability of a crash empirically. We now investigate whether these empirical successes survive the introduction of various stock characteristics, and compare the lower bound more directly with the forecasting performance of the risk-neutral probability of a crash.

We consider three categories of stock characteristics. The first category focuses on

Table 3: Validity and tightness of the option-implied crash probability bounds: the Back, Crotty, and Kazempour (2022) tests

This table reports p-values for tests of the validity and tightness of our proposed bounds, using the methodology described in Back, Crotty, and Kazempour (2022). The data are monthly from January 1996 to December 2022. Firms under consideration are S&P 500 constituents. The return horizons, denoted by τ, are one month, three months, six months, and one year. For $q = 0.80, 0.90$ and 0.95, define

$$\lambda = \mathbb{E}\left[\{\boldsymbol{I}(R_{i,t\to t+\tau} \leq q) - X_{it}(\tau, q)\}\, \boldsymbol{z}_t\right],$$

where X stands for $\mathbb{P}^L$ (the lower bounds), $\mathbb{P}^U$ (the upper bounds), or $\mathbb{P}^*$ (the risk-neutral probabilities); the elements of $\boldsymbol{z}_t$ are 1) a constant one, 2) the dividend yield of the market, 3) the earnings yield of the market, 4) the spread between five-year and three-month treasury yields, 5) the net equity issuance scaled by the market capitalization, 6) the month-to-month inflation rate, 7) the BAA-AAA credit spread, 8) the book-to-market ratio of the market, 9) the three-month treasury yield and 10) the VIX index. $H_0 : \lambda \geq 0$ vs. $H_1 : \lambda \in \mathbb{R}^d$ tests if a lower bound is valid; $H_0 : \lambda = 0$ vs. $H_1 : \lambda \geq 0$ tests if a lower bound is tight; $H_0 : \lambda \leq 0$ vs. $H_1 : \lambda \in \mathbb{R}^d$ tests if an upper bound is valid; $H_0 : \lambda = 0$ vs. $H_1 : \lambda \leq 0$ tests if an upper bound is tight.

	lower bound				upper bound			
horizon	1	3	6	12	1	3	6	12
Panel A: $q = 0.80$, down by over 20%								
validity	0.452	0.381	0.621	0.487	0.769	1.000	0.754	1.000
tightness	0.352	0.022	0.043	0.164	0.011	0.000	0.000	0.018
Panel B: $q = 0.90$, down by over 10%								
validity	0.069	0.626	0.683	0.505	0.780	0.768	0.755	0.755
tightness	0.133	0.059	0.057	0.114	0.000	0.000	0.000	0.020
Panel C: $q = 0.95$, down by over 5%								
validity	0.552	0.629	0.563	0.486	1.000	0.779	0.760	1.000
tightness	0.176	0.043	0.048	0.096	0.001	0.000	0.000	0.019

seven variables associated with the cross-section of expected stock returns: CAPM beta, relative size (the logarithms of a firm's market capitalization scaled by that of the S&P 500 index), book-to-market ratio, gross profitability (gross profits scaled by total assets), two momentum measures (stock returns from month -6 to month -1 and month -12 to month -1), and the most recent month's return (as a reversal signal).

The second category includes four stock characteristics that the prior literature has found useful in forecasting crashes: the volatility of market-adjusted returns and average monthly turnover (both of which are highlighted in Chen, Hong, and Stein (2001)), sales growth (Greenwood, Shleifer, and You, 2019), and short interest scaled by institutional ownership (Asquith, Pathak, and Ritter, 2005; Daniel, Klos, and Rottke, 2023).

The third category includes four variables motivated by the approach of Campbell, Hilscher, and Szilagyi (2008) to forecasting corporate bankruptcies and failures: the leverage (debt-to-asset) ratio, net income scaled by total assets, cash and short-term investment scaled by total assets, and log price per share. Appendix C gives further detail on the construction of all fifteen characteristics, and Table A1 presents summary statistics.

Table 4 reports results for a crash of at least 20% over the next month. To make it easier to assess the economic significance of the forecasting variables, we rescale the lower bound, the risk-neutral probability, and all stock characteristics to have unit standard deviation, and we multiply coefficient estimates by 100. As a result of this rescaling, each coefficient measures the influence, in percentage points, of a one standard deviation move in the relevant variable. Asterisks indicate coefficients whose t-statistics are greater than 4 in absolute value.[10]

The first column of the table reports results for a multivariate regression of the crash indicator variable onto the stock characteristics described above. Together, the characteristics achieve an R^2 of 4.51%. Two of the characteristics are highly significant: the volatility measure of Chen, Hong, and Stein (2001) has a t-statistic around 7, and short interest scaled by institutional ownership has a t-statistic above 4.

The second column shows that the lower bound, on its own, performs better than the stock characteristics do collectively. It explains more of the variation in crashes, with R^2 of 5.66%, and is highly statistically significant, with a t-statistic above 8. (This regression is identical, up to the rescaling, to the regression with an estimated coefficient of 0.92 reported in Panel A of Table 2.)

The third column reports results of a multivariate regression that uses both the lower

[10] We choose a high threshold to avoid false positives, as recommended by Harvey, Liu, and Zhu (2016).

Table 4: Regression tests of the option-implied crash probability bounds: adjusted regressions for 20% crash in one month

This table reports the results from the following regressions:

$$\boldsymbol{I}(R_{i,t\to t+1} \leq 0.80) = \beta \cdot X_{it}(\tau, 0.80) + \lambda \cdot \text{controls}_{it} + \varepsilon_{i,t+1},$$

in which X stands for $\mathbb{P}^L$ (the lower bounds), $\mathbb{P}^*$ (the risk-neutral probability), or both. The controls are fifteen firm characteristics from the literature. All independent variables are transformed to have a unit standard deviation. Regression coefficients are reported as percentage points, and their two-way clustered standard errors are included in the parentheses. The first five columns are simple OLS estimates, and the sixth column reports estimates with time fixed effects, with a projected (within) R^2 replacing the standard ones. Asterisks indicate coefficients whose t-statistics exceed four in magnitude.

	$\boldsymbol{I}(R_{t\to t+1} \leq 0.8)$					
	(1)	(2)	(3)	(4)	(5)	(6)
$\mathbb{P}^L[R_{t\to t+1} \leq 0.8]$		3.41*	3.05*		4.44	2.74*
		(0.41)	(0.59)		(3.08)	(0.33)
$\mathbb{P}^*[R_{t\to t+1} \leq 0.8]$				2.83*	−1.40	
				(0.67)	(3.37)	
beta	0.48		0.12	0.18	0.10	0.23
	(0.15)		(0.16)	(0.17)	(0.14)	(0.14)
relative size	0.07		−0.01	−0.03	0.00	0.09
	(0.10)		(0.10)	(0.10)	(0.10)	(0.08)
book-to-market	−0.18		−0.20	−0.20	−0.20	−0.07
	(0.11)		(0.11)	(0.11)	(0.11)	(0.08)
gross profit.	−0.14		−0.08	−0.10	−0.07	−0.04
	(0.09)		(0.09)	(0.09)	(0.08)	(0.07)
$r_{(t-1)\to t}$	−0.29		−0.09	−0.08	−0.11	−0.16
	(0.18)		(0.18)	(0.19)	(0.19)	(0.13)
$r_{(t-6)\to(t-1)}$	−0.45		−0.26	−0.25	−0.27	−0.35
	(0.20)		(0.20)	(0.20)	(0.20)	(0.17)
$r_{(t-12)\to(t-1)}$	−0.06		−0.07	−0.05	−0.08	−0.14
	(0.20)		(0.19)	(0.19)	(0.18)	(0.17)
CHS-volatility	2.28*		0.30	0.43	0.31	0.50
	(0.31)		(0.38)	(0.45)	(0.39)	(0.18)
turnover	0.18		−0.06	−0.07	−0.05	0.08
	(0.27)		(0.25)	(0.24)	(0.24)	(0.15)
sales growth	0.21		0.20	0.21	0.20	0.13
	(0.11)		(0.11)	(0.11)	(0.11)	(0.08)
short int.	0.39*		0.33*	0.36*	0.32*	0.27*
	(0.09)		(0.08)	(0.08)	(0.08)	(0.06)
leverage	−0.15		−0.10	−0.13	−0.09	−0.07
	(0.12)		(0.12)	(0.12)	(0.11)	(0.11)
net income/asset	−0.21		−0.14	−0.17	−0.13	−0.14
	(0.12)		(0.12)	(0.12)	(0.11)	(0.08)
cash/asset	−0.09		−0.09	−0.08	−0.09	−0.03
	(0.08)		(0.08)	(0.08)	(0.08)	(0.07)
log price	−0.33		0.14	0.06	0.16	0.07
	(0.16)		(0.15)	(0.15)	(0.17)	(0.13)
intercept	0.04	0.00	−0.03	−0.01	−0.03	
	(0.03)	(0.00)	(0.03)	(0.03)	(0.03)	
R^2/R^2-proj.	4.51%	5.66%	5.85%	5.72%	5.87%	4.74%

bound and the stock characteristics to forecast crashes. The lower bound remains highly significant, with a t-statistic above 5. Of the stock characteristics, only short interest remains statistically significant, and the collective marginal contribution to explanatory power of the characteristics is small. The coefficient on the lower bound is roughly an order of magnitude greater than that on short interest: a one standard deviation move in the lower bound moves the implied crash probability by 3.05 percentage points, whereas a one standard deviation move in short interest moves the implied crash probability by 0.33 percentage points.

Columns (4) and (5) of the tables include the risk-neutral probability of a crash, either alone as an alternative to the lower bound, or together with it. At all three horizons, the risk-neutral probability enters strongly significantly when included on its own, but achieves a lower R^2 than the lower bound does. When both are included together, the coefficient on the lower bound is positive while that on the risk-neutral probability is negative; but the coefficients are imprecisely estimated, as the lower bound and risk-neutral probability are highly correlated.

Tables A6 and A7, in the Appendix, report similar results over horizons of one quarter and one year, respectively. As before, we rescale all right-hand side variables to have unit standard deviation so that coefficient estimates indicate the economic importance of the various potential predictors. The lower bound remains highly significant both in statistical (the t-statistic is large) and economic (the estimated coefficient is large) terms. In the univariate regression at the one-year horizon, for example, a one standard deviation increase in the lower bound represents a 6.96 percentage point increase in the probability of a crash, with a t-statistic above 12. When all stock characteristics are included, the coefficient estimate drops to 5.28, with a t-statistic above 7. The stock characteristics are somewhat more informative at this longer horizon: sales growth and short interest are highly statistically significant with estimated coefficients of 1.86 and 2.28, respectively.

3.2 Out-of-sample forecasts

We now explore whether the lower bound performs well out of sample by using it as a direct forecaster of crashes—that is, forcing the coefficients α and β in (7) to equal zero and one, respectively, so that no parameters need to be estimated.

3.2.1 Comparison to historical averages

We first compare the lower bound to two natural benchmarks: the average historical crash probability of all firms in our sample (a simple model which, at a given point in time, makes the same prediction for all stocks), and the average historical crash probability for stock i.

We assess relative performance of the bound versus these two models using the out-of-sample R^2 measures

$$R^2_{\text{oos, full-sample}} = 1 - \frac{\sum_t \sum_i \left\{ \boldsymbol{I}(R_{i,t\to t+\tau} \leq 0.8) - \mathbb{P}^L_t \left[R_{i,t\to t+\tau} \leq 0.8 \right] \right\}^2}{\sum_t \sum_i \left\{ \boldsymbol{I}(R_{i,t\to t+\tau}, 0.8) - p_t \right\}^2} \tag{8}$$

and

$$R^2_{\text{oos, firm-specific}} = 1 - \frac{\sum_t \sum_i \left\{ \boldsymbol{I}(R_{i,t\to t+\tau} \leq 0.8) - \mathbb{P}^L_t \left[R_{i,t\to t+\tau} \leq 0.8 \right] \right\}^2}{\sum_t \sum_i \left\{ \boldsymbol{I}(R_{i,t\to t+\tau}, 0.8) - p_{i,t} \right\}^2}, \tag{9}$$

where τ denotes the forecasting horizon; $\mathbb{P}^L_t \left[R_{i,t\to t+\tau} \leq 0.8 \right]$ is the lower bound on the true probability of a 20% crash; p_t is the historical average crash probability estimated over the period from 1 to $(t - \tau)$ across all firms in the sample; and $p_{i,t}$ is the corresponding historical average crash probability for firm i.

We also repeat these exercises for the risk-neutral probabilities (i.e., replacing $\mathbb{P}^L_t \left[R_{i,t\to t+\tau} \leq 0.8 \right]$ with $\mathbb{P}^*_t \left[R_{i,t\to t+\tau} \leq 0.8 \right]$ in (8) and (9) above).

Figure 3 plots the R^2_{oos} measures, calculated over expanding windows. The lower bound outperforms the two historical averages at all horizons, with R^2_{oos} around 5% to 10%. Moreover, the outperformance is fairly consistent over time, as opposed to being concentrated on a particular market episode. The risk-neutral probability does poorly by comparison, with performance similar to that of the full-sample average at forecasting horizons of six month or one year.

3.2.2 Comparison to characteristics-based models

To generate more a challenging competitor variable, we design a procedure to emulate an avid "data-snooper". We split the dataset into a training and a testing sample, and present results for three different choices—2006, 2011, and 2016—of cutoff year. The fifteen stock characteristics considered in Section 3.1.3 and the risk-neutral crash probability are combined through linear and logistic regressions to forecast crash events; in each case, we report results using only the fifteen stock characteristics, and using the fifteen stock

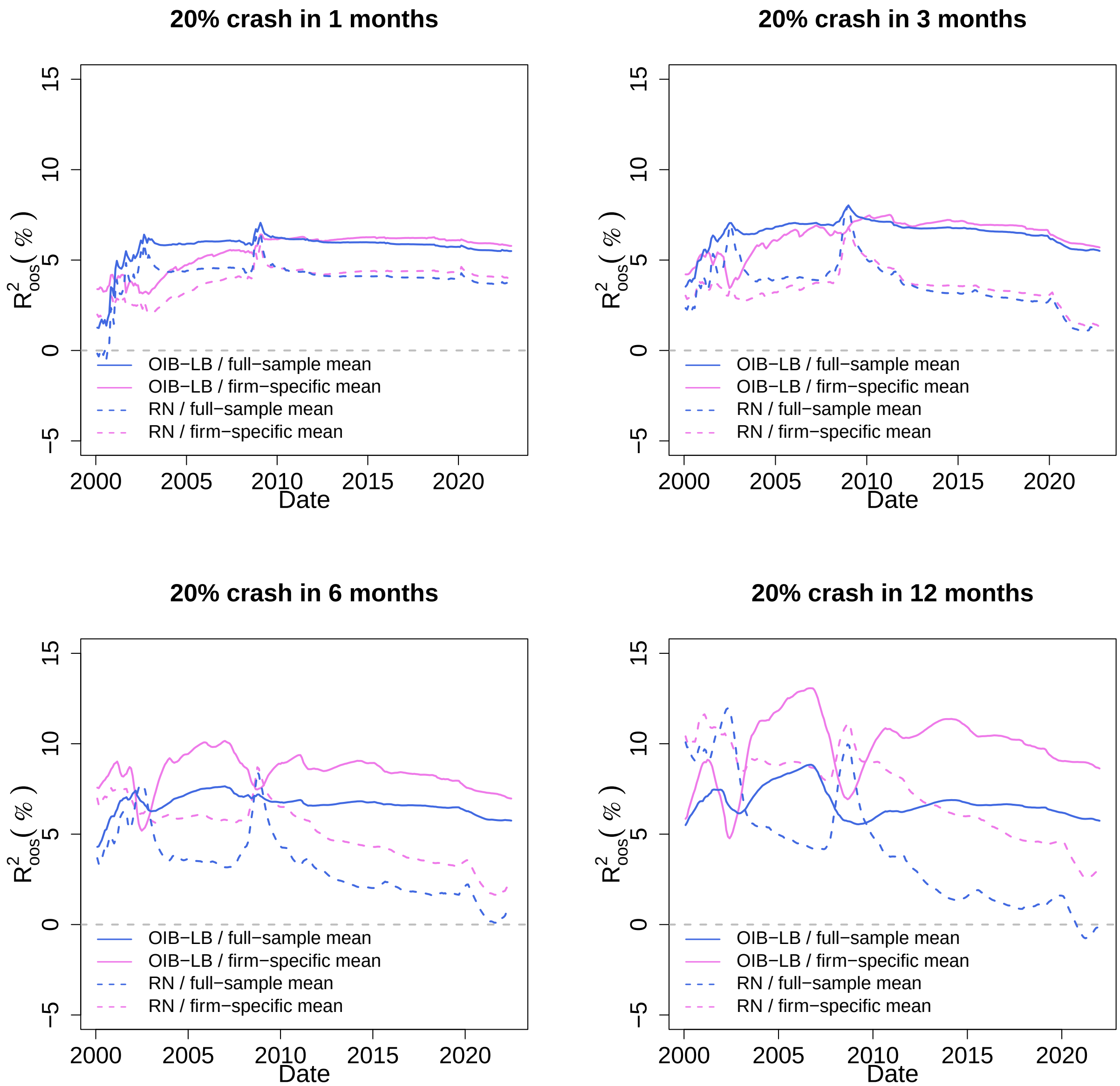

Figure 3: Out-of-sample R^2s.

This figure presents the out-of-sample R^2s for our option-implied lower bounds (OIB-LB) and the risk-neutral probabilities (RN). For any time point t, the sum of squared forecasting errors using OIB-LB or RN is compared against the sum of forecasting errors using full-sample or firm-specific average probability of crashes through period $1 : (t - \tau)$, where $\tau(= 1, 3, 6, 12)$ represents the forecasting horizon.

characteristics plus the risk-neutral probability. We fit these models in the training sample and select the best model through cross-validation using the LASSO approach.

Figure 4 compares the resulting models with the lower bound in their ability to forecast individual stock crashes at the one-month and one-year horizons. It plots the ROC curves as a measure of forecasting performance that balances type-I and type-II forecasting errors. On this diagram, the ROC curve for a random (i.e., totally uninformative) predictor variable would be a 45 degree line; at the opposite extreme, the ROC curve for an oracle (i.e., a perfect predictor of the future) would rise vertically to a true positive fraction of 1 at a false positive fraction of 0. More generally, superior predictors have ROC curves shifted toward the top-left of the diagram. As is clear, the lower bound outperforms the logistic LASSO and OLS LASSO models, particularly at the one-month horizon.

Table A8 reports the area under the ROC curves (AUC). A higher AUC indicates better predictive performance. The lower bound dominates the LASSO models. The three choices of cutoff year and four horizons give 12 AUC statistics for each model, and the (univariate) lower bound outperforms the other (multivariate) models in all 12 cases.

4 Bounds for general contingent payoffs

Result 1, which underpins our empirical work, requires that the function $g(x,y) = x^\gamma h(y)$ is two-increasing. When this is not the case, we can modify our approach by exploiting a result of Hofer and Iacò (2014). Specifically, for any well-behaved function k,

$$\max_{C\in\mathcal{C}} \int_{[0,1]^2} k\left(u,v\right)\,\mathrm{d}C(u,v) \approx \max_{\pi\in\mathcal{P}_n} \frac{1}{n}\sum_{i=1}^{n} k\left(\frac{i}{n},\frac{\pi(i)}{n}\right) \tag{10}$$

where $\mathcal{P}_n$ is the set of permutations of $\{1,\dots,n\}$, and the approximate equality can be made to hold up to arbitrarily small error by choosing n sufficiently large. The two conditions on k are that (i) it must be such that the integral is finite and (ii) it must be Lipschitz continuous almost everywhere.

The right-hand side of (10) is the canonical linear assignment problem in combinatorial optimization. The so-called Hungarian algorithm (Kuhn, 1955) reduces the complexity of solving this problem from $O(n!)$ (based on brute-force search) to $O(n^3)$. Similarly, to obtain lower bounds, we can apply the Hungarian algorithm to the integral involving $-k(u,v)$. Using this approach, together with Sklar's theorem, we have the following result.

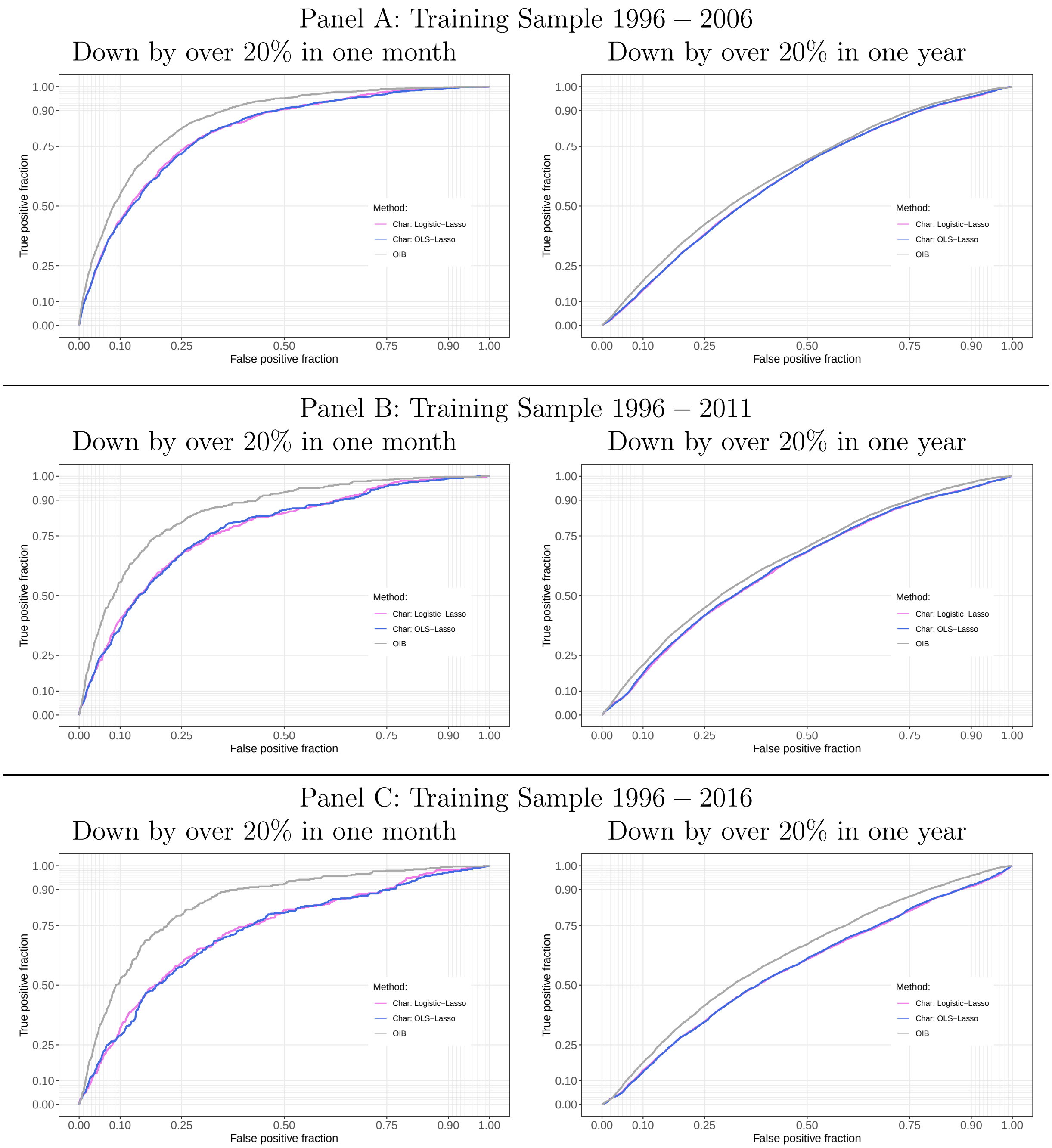

Figure 4: Out-of-sample forecasting of crash events: ROC curves from the option-implied lower bounds (OIB) vs. characteristics-based statistical models

The figures above show ROC curves for forecasts of 20% crashes in a month or a year, using the option-implied lower bounds (OIB-LB) and linear and logistic regressions with variables selected by the Lasso (OLS-Lasso and Logistic-Lasso).

Result 6. *Let h be Lipschitz continuous almost everywhere. If $\pi_{\min}$ is a permutation of $\{1,\ldots,n\}$ that minimizes $\sum_{k=1}^{n} k\left(\frac{i}{n},\frac{\pi(i)}{n}\right)$ and $\pi_{\max}$ is a permutation that maximizes $\sum_{k=1}^{n} k\left(\frac{i}{n},\frac{\pi(i)}{n}\right)$, then (up to errors that can be made arbitrarily small by choosing n sufficiently large)*

$$\frac{1}{nC}\sum_{i=1}^{n} k\left(\frac{i}{n},\frac{\pi_{\min(i)}}{n}\right) \leq \mathbb{E}[h(R_i)] \leq \frac{1}{nC}\sum_{i=1}^{n} k\left(\frac{i}{n},\frac{\pi_{\max(i)}}{n}\right),$$

where the constant C equals $\int_0^1 [Q_m^{-1}(u)]^{\gamma}\,\mathrm{d}u$ and $k(u,v)=g\left(Q_m^{-1}(u),\,Q_i^{-1}(v)\right)$.

As a simple example, if we are interested in evaluating the probability that a stock's return lies in some interval, Result 6 can be applied with $h(R_i)=\boldsymbol{I}(q_1\leq R_i\leq q_2)$.

5 Conclusion

We introduce a new forecasting variable that exploits information in option prices, and which successfully predicts crashes in individual stocks. We do so as part of a more general framework that supplies bounds on the expectation of a general function of the market return and of an individual asset return.

We could, of course, use option prices in a straightforward way to calculate *risk-neutral* probabilities of crashes. This approach is widely used by practitioners, and it has an appealing simplicity. On the other hand, as is well understood, we should expect such a measure to overstate the probability of a crash, as risk-neutral probabilities put extra weight on bad outcomes. We confirm this expectation in the data.

We would therefore like to move from risk-neutral probabilities to the *true* probabilities in which we are ultimately interested. We rely on an assumption on the form of the SDF to do so, namely that it is a power of the return on the the market, as in an equilibrium model in which a myopic investor with power utility chooses to hold the market.

Even after making the power utility assumption, we face a further problem: to use option prices to measure the true probability that a given stock crashes, we need to understand the joint risk-neutral distribution of that stock and the market. But the prices we observe—of options on the market and of options on individual stocks—only reveal the *univariate* risk-neutral distributions of the market and of the individual stocks.

We solve this problem with the final theoretical ingredient of the paper, the Fréchet–Hoeffding theorem, which places bounds on the relationship between the joint distribution and the marginal distributions that are tighter than those derived from the Cauchy–Schwarz inequality. We use the theorem to derive upper and lower bounds on the probability that an individual stock crashes, and show theoretically (and confirm empirically) that the upper and lower bounds are, respectively, higher and lower than the risk-neutral probability that the given stock crashes.

The lower bound is tight if the return on the stock in question is a (potentially nonlinear) monotonic increasing function of the return on the market; correspondingly, the upper bound would be tight if the stock return were a monotonic decreasing function of the market return. The former is the more empirically plausible case, and indeed we find, across forecasting horizons and crash sizes, that the lower bound is a highly statistically significant forecaster of crashes. We find, moreover, that the estimated coefficient is close to one, as it should be if the lower bound is a good proxy for the true crash probability. (The upper bound and risk-neutral probability are also significant predictors of crashes, but they enter with coefficients significantly less than one, as theory would lead us to expect, and they achieve lower R^2 than the lower bound does.)

When we conduct formal tests of the validity and tightness of the bounds, following Back et al. (2022), we do not reject their validity. We can, as expected, strongly reject the hypothesis that the upper bound is tight. The evidence on the tightness of the lower bound is not decisive.

We compare the in- and out-of-sample performance of the lower bound with fifteen stock characteristics suggested by the prior literature, and with the risk-neutral probability of a crash. The lower bound is a highly significant forecaster of crashes at all horizons, and it drives out variables such as beta and realized volatility. Indeed, at the one-month and one-quarter horizons, the lower bound *on its own* outperforms the fifteen characteristics and the risk-neutral probability *combined.*

References

Aït-Sahalia, Y. and A. W. Lo (1998). Nonparametric estimation of state-price densities implicit in financial asset prices. *Journal of Finance 53*(2), 499–547.

Ang, A., J. Chen, and Y. Xing (2006). Downside risk. *Review of Financial Studies 19*(4), 1191–1239.

Asquith, P., P. A. Pathak, and J. R. Ritter (2005). Short interest, institutional ownership, and stock returns. *Journal of Financial Economics 78*(2), 243–276.

Back, K., K. Crotty, and S. M. Kazempour (2022). Validity, tightness, and forecasting power of risk premium bounds. *Journal of Financial Economics 144*, 732–760.

Bates, D. S. (1991). The crash of '87: Was it expected? The evidence from options markets. *Journal of Finance 46*(3), 1009–1044.

Boyer, B., T. Mitton, and K. Vorkink (2009). Expected idiosyncratic skewness. *Review of Financial Studies 23*(1), 169–202.

Breeden, D. T. and R. H. Litzenberger (1978). Prices of state-contingent claims implicit in option prices. *Journal of Business 51*(4), 621–651.

Campbell, J. Y., J. Hilscher, and J. Szilagyi (2008). In search of distress risk. *Journal of Finance 63*(6), 2899–2939.

Carr, P. and D. Madan (2001). Towards a theory of volatility trading. In E. Jouini, J. Cvitanić, and M. Musiela (Eds.), *Handbooks in Mathematical Finance: Option Pricing, Interest Rates and Risk Management*, pp. 458–476. Cambridge University Press.

Carr, P. and L. Wu (2009). Variance risk premiums. *Review of Financial Studies 22*(3), 1311–1341.

Chabi-Yo, F., C. Dim, and G. Vilkov (2023). Generalised bounds on the conditional expected excess return on individual stocks. *Management Science 69*(2), 922–939.

Chabi-Yo, F. and J. Loudis (2020). The conditional expected market return. *Journal of Financial Economics 137*(3), 752–786.

Chen, J., H. Hong, and J. C. Stein (2001). Forecasting crashes: Trading volume, past returns, and conditional skewness in stock prices. *Journal of Financial Economics 61*(3), 345–381.

Christoffersen, P., M. Fournier, and K. Jacobs (2018). The factor structure in equity options. *Review of Financial Studies 31*(2), 595–637.

Christoffersen, P., K. Jacobs, and B. Y. Chang (2013). Forecasting with option-implied information. In G. Elliott and A. Timmermann (Eds.), *Handbook of Economic Forecasting*, Volume 2, pp. 581–656. Elsevier.

Daniel, K., A. Klos, and S. Rottke (2023). The dynamics of disagreement. *Review of Financial Studies 36*(6), 2431–2467.

Della Corte, P., C. Gao, and A. Jeanneret (2023). Expected currency returns and term structure of risk preferences. working paper.

Driscoll, J. C. and A. C. Kraay (1998). Consistent covariance matrix estimation with spatially dependent panel data. *Review of Economics and Statistics 80*(4), 549–560.

Gandhi, M., N. J. Gormsen, and E. Lazarus (2022). Does the market understand time variation in the equity premium? working paper.

Gao, C. and I. W. R. Martin (2021). Volatility, valuation ratios, and bubbles: An empirical measure of market sentiment. *Journal of Finance 76*(6), 3211–3254.

Gao, X. and J. R. Ritter (2010). The marketing of seasoned equity offerings. *Journal of Financial Economics 97*(1), 33–52.

Goetzmann, W. N., D. Kim, and R. J. Shiller (2022). Crash narratives. NBER Working Paper 30195.

Greenwood, R., A. Shleifer, and Y. You (2019). Bubbles for Fama. *Journal of Financial Economics 131*(1), 20–43.

Harvey, C. R., Y. Liu, and H. Zhu (2016). . . . and the cross-section of expected returns. *Review of Financial Studies 29*(1), 5–68.

Hofer, M. and M. R. Iacò (2014). Optimal bounds for integrals with respect to copulas and applications. *Journal of Optimization Theory and Applications 3*, 999–1011.

Jackwerth, J. C. and M. Rubinstein (1996). Recovering probability distributions from option prices. *Journal of Finance 51*(5), 1611–1631.

Kadan, O. and X. Tang (2020). A bound on expected stock returns. *Review of Financial Studies 33*(4), 1565–1617.

Kelly, B. and H. Jiang (2014). Tail risk and asset prices. *Review of Financial Studies 27*(10), 2841–2871.

Kelly, B., H. Lustig, and S. Van Nieuwerburgh (2016). Too-systemic-to-fail: What option markets imply about sector-wide government guarantees. *American Economic Review 106*(6), 1278–1319.

Kremens, L. and I. W. R. Martin (2019). The quanto theory of exchange rates. *American Economic Review 109*(3), 810–843.

Kuhn, H. W. (1955). The Hungarian method for the assignment problem. *Naval Research Logistics 2*(1-2), 83–97.

Martin, I. W. R. (2017). What is the expected return on the market? *Quarterly Journal of Economics 132*(1), 367–433.

Martin, I. W. R. (2018). Options and the gamma knife. *Journal of Portfolio Management 44*(6), 47–55.

Martin, I. W. R. (2021). On the autocorrelation of the stock market. *Journal of Financial Econometrics 19*(1), 39–52.

Martin, I. W. R. and C. Wagner (2019). What is the expected return on a stock? *Journal of Finance 74*(4), 1887–1929.

Pederzoli, P. (2021). Skewness swaps: Evidence from the cross-section of stocks. Working paper.

Ross, S. A. (1976). Options and efficiency. *Quarterly Journal of Economics 90*(1), 75–89.

Rubinstein, M. (1994). Implied binomial trees. *Journal of Finance 49*(3), 771–818.

Sklar, A. (1959). Fonctions de répartition à n dimensions et leurs marges. *Publ. Inst. Statist. Univ. Paris 8*, 229–231.

Tchen, A. H. (1980). Inequalities for distributions with given marginals. *Annals of Probability 8*(4), 814–827.

Thompson, S. B. (2011). Simple formulas for standard errors that cluster by both firm and time. *Journal of Financial Economics 99*(1), 1–10.

Tibshirani, R. (1996). Regression shrinkage and selection via the lasso. *Journal of the Royal Statistical Society: Series B (Methodological) 58*(1), 267–288.

Vilkov, G. and Y. Xiao (2013). Option-implied information and predictability of extreme returns. working paper.

Welch, I. and A. Goyal (2008). A comprehensive look at the empirical performance of equity premium prediction. *Review of Financial Studies 21*(4), 1455–1508.

A Proofs

A.1 Proof of Result 1

Proof. When $g(x, y)$, defined on $[0, \infty)\times[0, \infty)$, is continuous and two-increasing, $k(u, v) = g\left(Q_m^{-1}(u),\, Q_i^{-1}(v)\right)$ is two-increasing in $[0, 1] \times [0, 1]$. We therefore have

$$\inf_{C\in\mathcal{C}} \int_{[0,1]^2} k\,(u, v)\ \mathrm{d}C(u, v) \le \int g\,(x, y)\ \mathrm{d}Q_{mi}(x, y) \le \sup_{C\in\mathcal{C}} \int_{[0,1]^2} k\,(u, v)\ \mathrm{d}C(u, v), \tag{11}$$

where we write $\mathcal{C}$ for the set of all two-dimensional copulas, and

$$k(u, v) = g\left(Q_m^{-1}(u),\, Q_i^{-1}(v)\right). \tag{12}$$

From Corollary 2.2 of Tchen (1980), we have

$$\inf_{C\in\mathcal{C}} \int_{[0,1]^2} k(u, v)\,\mathrm{d}C(u, v) = \int_{[0,1]^2} k(u, v)\,\mathrm{d}\left(\max(u + v - 1,\ 0)\right),$$

and

$$\sup_{C\in\mathcal{C}} \int_{[0,1]^2} k(u, v)\,\mathrm{d}C(u, v) = \int_{[0,1]^2} k(u, v)\,\mathrm{d}\left(\min(u, v)\right).$$

The probability densities of the Fréchet–Hoeffding lower bound, $\max(u + v - 1,\ 0)$, and the Fréchet–Hoeffding upper bound, $\min(u, v)$, are uniformly distributed along the two diagonals of the square $[0, 1]^2$ in $\mathbb{R}^2$, illustrated as follows:

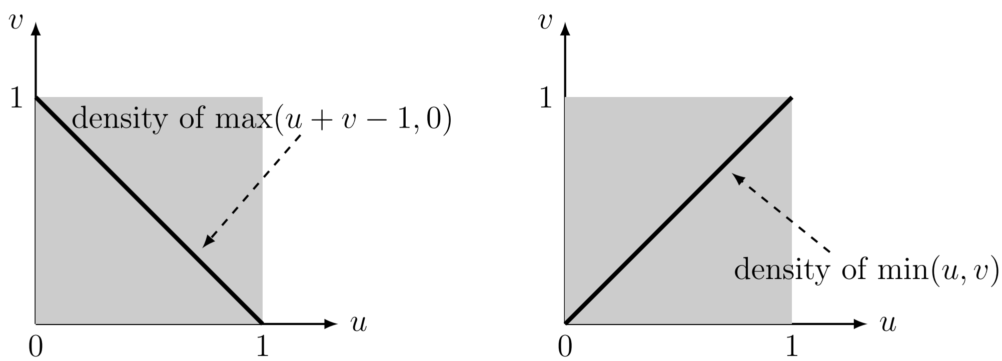

Integrating the right-hand sides of the two equations above (with regard to these two densities), we have

$$\int_{[0,1]^2} k(u,v)\,\mathrm{d}\left(\max(u+v-1,\ 0)\right) = \int_0^1 k(u,1-u)\,\mathrm{d}u$$

and

$$\int_{[0,1]^2} k(u,v)\,\mathrm{d}\left(\min(u,v)\right) = \int_0^1 k(u,u)\,\mathrm{d}u.$$

Substituting these expressions back into (11) and using the definition (12) of $k(u,v)$, it follows that

$$\int_0^1 g\left(Q_m^{-1}(u),\, Q_i^{-1}(1-u)\right)\,\mathrm{d}u \le \int g\left(x,y\right)\,\mathrm{d}Q_{mi}(x,y) \le \int_0^1 g\left(Q_m^{-1}(u),\, Q_i^{-1}(u)\right)\,\mathrm{d}u\,.$$

The result follows on making the change of variable $R_m = Q_m^{-1}(u)$ in the left- and right-most integrals. $\square$

A.2 Proof of Result 2

Proof. Under the stated assumptions, the function $g(x,y) = x^\gamma h(y)$ is continuous and two-increasing. From Result 1, we have

$$\int_0^1 \left[Q_m^{-1}(1-u)\right]^\gamma h\left(Q_i^{-1}(u)\right)\,\mathrm{d}u \le \mathbb{E}^*[R_m^\gamma h(R_i)] \le \int_0^1 \left[Q_m^{-1}(u)\right]^\gamma h\left(Q_i^{-1}(u)\right)\,\mathrm{d}u.$$

Making the change of variables $R_m = Q_m^{-1}(u)$, it follows that

$$\int_0^1 \left[Q_m^{-1}(u)\right]^\gamma h\left(Q_i^{-1}(1-u)\right)\,\mathrm{d}u = \int_0^\infty R_m^\gamma h(Q_i^{-1}(1-Q_m(R_m)))\,\mathrm{d}Q_m(R_m)$$

and

$$\int_0^1 \left[Q_m^{-1}(u)\right]^\gamma h\left(Q_i^{-1}(u)\right)\,\mathrm{d}u = \int_0^\infty R_m^\gamma h(Q_i^{-1}(Q_m(R_m)))\,\mathrm{d}Q_m(R_m),$$

which give the bounds stated in the result.

The lower bound is achieved when the copula linking Q_m and Q_i is $\max(u+v-1,\,0)$, that is, the joint risk-neutral CDF of $(Q_m(R_m), Q_i(R_i))$ is $\max(u+v-1,0)$. This implies that $Q_m(R_m) + Q_i(R_i) \equiv 1$. Similarly, the upper bound is achieved when the joint risk-neutral CDF of $(Q_m(R_m), Q_i(R_i))$ is $\min(u,v)$, that is, when $Q_i(R_i) = Q_m(R_m)$. $\square$

A.3 Proof of Result 3

Proof. Setting $h(R_i) = -\boldsymbol{I}(R_i \le q)$ in Result 2, we have

$$\begin{aligned}
\mathbb{P}[R_i \le q] &= -\,\mathbb{E}[h(R_i)] \\
&\ge -\,\frac{\mathbb{E}^*\left[R_m^\gamma h(Q_i^{-1}(Q_m(R_m)))\right]}{\mathbb{E}^*\left[R_m^\gamma\right]} \\
&= \frac{\mathbb{E}^*\left[R_m^\gamma \boldsymbol{I}(Q_m(R_m) \le Q_i(q))\right]}{\mathbb{E}\left[R_m^\gamma\right]} \\
&= \frac{\mathbb{E}^*\left[R_m^\gamma \boldsymbol{I}\left(R_m \le q_l\right)\right]}{\mathbb{E}\left[R_m^\gamma\right]} \qquad \left(q_l = Q_m^{-1}\left(Q_i\left(q\right)\right) \text{ by definition}\right).
\end{aligned}$$

The inequality holds with equality if and only if R_m and R_i are comonotonic—that is, one is a monotonically increasing function of the other—so that $Q_i(R_i) = Q_m(R_m)$. Similarly, we have

$$\begin{aligned}
\mathbb{P}[R_i \le q] &= -\mathbb{E}[h(R_i)] \\
&\le -\frac{\mathbb{E}^*\left[R_m^\gamma h(Q_i^{-1}(1 - Q_m(R_m)))\right]}{\mathbb{E}^*\left[R_m^\gamma\right]} \\
&= \frac{\mathbb{E}^*\left[R_m^\gamma \boldsymbol{I}\left(1 - Q_m(R_m) \le Q_i(q)\right)\right]}{\mathbb{E}^*\left[R_m^\gamma\right]} \\
&= \frac{\mathbb{E}^*\left[R_m^\gamma \boldsymbol{I}\left(R_m \ge q_u\right)\right]}{\mathbb{E}^*\left[R_m^\gamma\right]} \qquad \left(q_u = Q_m^{-1}\left(1 - Q_i\left(q\right)\right) \text{ by definition}\right).
\end{aligned}$$

Again, the inequality in the second step can be strictly equal if and only if R_m and R_i are coutermonotonic—that is, one is a monotonically decreasing function of the other—so that $Q_i(R_i) = 1 - Q_m(R_m)$.

The upper bound is always greater than the lower bound. A bridge between them is the *risk-neutral* crash probability. Specifically, by the continuous version of Chebyshev's sum inequality,[11]

$$\frac{\mathbb{E}^*\left[R_m^\gamma \boldsymbol{I}\left(R_m \le q_l\right)\right]}{\mathbb{E}\left[R_m^\gamma\right]} \le \frac{\mathbb{E}^*\left[R_m^\gamma\right]\mathbb{E}^*\left[\boldsymbol{I}\left(R_m \le q_l\right)\right]}{\mathbb{E}^*\left[R_m^\gamma\right]} = Q_m(q_l) = Q_i(q) = \mathbb{P}^*[R_i \le q]$$

[11] This inequality states that for functions f and g which are integrable over $[0,1]$, both non-increasing or both non-decreasing, then $\int_0^1 f(x)g(x)\,\mathrm{d}x \ge \int_0^1 f(x)\,\mathrm{d}x \int_0^1 g(x)\,\mathrm{d}x$. If one function is non-increasing and the other is non-decreasing, the inequality is reversed. Letting $f(x) = [Q_m^{-1}(x)]^\gamma$ (a non-decreasing function of x), we derive the first inequality by setting $g(x) = \boldsymbol{I}(x \le Q_i(q))$ and the second by setting $g(x) = \boldsymbol{I}(x \ge Q_i(q))$.

and

$$\frac{\mathbb{E}^*\left[R_m^\gamma \boldsymbol{I}\left(R_m \geq q_u\right)\right]}{\mathbb{E}^*\left[R_m^\gamma\right]} \geq \frac{\mathbb{E}^*\left[R_m^\gamma\right] \mathbb{E}^*\left[\boldsymbol{I}\left(R_m \geq q_u\right)\right]}{\mathbb{E}^*\left[R_m^\gamma\right]} = 1 - Q_m(q_u) = Q_i(q) = \mathbb{P}^*[R_i \leq q]. \quad \square$$

A.4 Proof of Result 4

Proof. When $\gamma = 0$, the bounds become $\mathbb{P}^*[R_m \leq q_l] \leq \mathbb{P}[R_i \leq q] \leq \mathbb{P}^*[R_m \geq q_u]$. By definition, both the lower and upper bounds equal $\mathbb{P}^*[R_i \leq q]$.

To show that the lower bound is decreasing in γ, define the (decreasing) function $\psi(x) = \boldsymbol{I}(Q_m(x) \leq Q_i(q))$. The lower bound is then $\mathbb{E}^*[R_m^\gamma \psi(R_m)]/\mathbb{E}^*[R_m^\gamma]$ and

$$\begin{aligned}
&\frac{\mathrm{d}}{\mathrm{d}\gamma}\left\{\frac{\mathbb{E}^*[R_m^\gamma \psi(R_m)]}{\mathbb{E}^*[R_m^\gamma]}\right\} \\
&= \frac{\mathbb{E}^*[R_m^\gamma \log(R_m)\psi(R_m)]\mathbb{E}^*[R_m^\gamma] - \mathbb{E}^*[R_m^\gamma \psi(R_m)]\mathbb{E}^*[R_m^\gamma \log(R_m)]}{\{\mathbb{E}^*[R_m^\gamma]\}^2} \\
&= \frac{1}{\{\mathbb{E}^*[R_m^\gamma]\}^2} \iint \left[x^\gamma \log(x)\psi(x) y^\gamma - x^\gamma \psi(x) y^\gamma \log(y)\right] \mathrm{d}Q_m(x)\,\mathrm{d}Q_m(y) \\
&\leq \frac{1}{\{\mathbb{E}^*[R_m^\gamma]\}^2}\left[\iint_{x \geq y \geq 0} x^\gamma y^\gamma \psi(y) \log\left(\frac{x}{y}\right) \mathrm{d}Q_m(x)\,\mathrm{d}Q_m(y)\right. \\
&\qquad\qquad \left. + \iint_{0 \leq x \leq y} x^\gamma y^\gamma \psi(x) \log\left(\frac{x}{y}\right) \mathrm{d}Q_m(x)\,\mathrm{d}Q_m(y)\right] \\
&= \frac{1}{\{\mathbb{E}^*[R_m^\gamma]\}^2}\left[\iint_{0 \leq x \leq y} x^\gamma y^\gamma \psi(x) \log\left(\frac{y}{x}\right) \mathrm{d}Q_m(x)\,\mathrm{d}Q_m(y)\right. \\
&\qquad\qquad \left. + \iint_{0 \leq x \leq y} x^\gamma y^\gamma \psi(x) \log\left(\frac{x}{y}\right) \mathrm{d}Q_m(x)\,\mathrm{d}Q_m(y)\right] \\
&= 0.
\end{aligned}$$

(The inequality follows because $\psi(x) \leq \psi(y)$ if $x \geq y$.) Thus the lower bound is decreasing with regard to the risk aversion parameter γ.

Applying the same logic to the increasing function $\psi(x) = \boldsymbol{I}(Q_m(x) \geq 1 - Q_i(q))$, we conclude that the upper bound is increasing with regard to γ.

Next, note that the lower bound is such that

$$\frac{\mathbb{E}^*\left[R_m^\gamma \boldsymbol{I}\left(R_m \leq q_l\right)\right]}{\mathbb{E}\left[R_m^\gamma\right]} \leq \frac{q_l^\gamma}{\mathbb{E}^*[R_m^\gamma]}.$$

To show that the lower bound converges to zero, we must show that $\mathbb{E}^*[(R_m/q_l)^\gamma] \to \infty$ as $\gamma \to \infty$. This holds if $\mathbb{P}^*[R_m/q_l > 1] > 0$. If this condition does not hold, $R_m \le q_l = Q_m^{-1}(Q_i(q))$ with probability one, which violates the assumption that $Q_i(q) < 1$. Thus, $\mathbb{E}^*[(R_m/q_l)^\gamma] \to \infty$ and the lower bound converges to zero as $\gamma \to \infty$.

To show that the upper bound goes to one as $\gamma \to \infty$, note that

$$1 = \frac{\mathbb{E}^*[R_m^\gamma \boldsymbol{I}(R_m < q_u)] + \mathbb{E}^*[R_m^\gamma \boldsymbol{I}(R_m \ge q_u)]}{\mathbb{E}^*[R_m^\gamma]}.$$

The result will therefore follow if we can show that $\mathbb{E}^*[R_m^\gamma \boldsymbol{I}(R_m < q_u)]/\mathbb{E}^*[R_m^\gamma] \to 0$ as $\gamma \to \infty$. Again, this is satisfied when $\mathbb{P}^*[R_m/q_u > 1] > 0$. If not, we would have $R_m \le q_u = Q_m^{-1}(1 - Q_i(q))$, and hence $1 - Q_i(q) = 1$; but this violates the assumption that $Q_i(q) > 0$. $\square$

A.5 Proof of Result 5

Proof. By the Carr–Madan formula (Carr and Madan, 2001), for any smooth function $g(\cdot)$ we have

$$g(S) = g(F) + g'(F)(S-F) + \int_0^F g''(K)\max\{K-S,\, 0\}\,\mathrm{d}K + \int_F^\infty g''(K)\max\{S-K,\, 0\}\,\mathrm{d}K.$$

Let S_0 and $F = S_0 R_f$ be the spot and forward level of the market index, the function $g(S)$ be S^γ. Treating S, a random variable, as the level of market index next period, taking the risk-neutral expectations on both sides of the equation above (changing orders of integrals when needed), we have

$$\begin{aligned}\mathbb{E}^*\left[S^\gamma\right] =& S_0^\gamma R_f^\gamma + \gamma S_0^{\gamma-1} R_f^{\gamma-1}(\mathbb{E}^*[S] - F) \\ &+ \int_0^F \gamma(\gamma-1)K^{\gamma-2} R_f \mathrm{put}(K)\,\mathrm{d}K + \int_F^\infty \gamma(\gamma-1)K^{\gamma-2} R_f \mathrm{call}(K)\,\mathrm{d}K.\end{aligned}$$

Dividing both sides by S_0^γ and noticing that $R_m = S/S_0$ and that $\mathbb{E}^*[S] = F$, we have the first equation.

Next, noticing that

$$\mathbb{E}^*\left[R_m^\gamma \boldsymbol{I}(R_m \le q_l)\right] = \frac{\mathbb{E}^*\left[S^\gamma \boldsymbol{I}(S \le K_l)\right]}{S_0^\gamma} = \frac{R_f}{S_0^\gamma}\int_0^{K_l} K^\gamma \mathrm{put}''(K)\,\mathrm{d}K$$

where the second equation follows by static replication logic (Breeden and Litzenberger, 1978). Integrating the last integral by parts and using the fact that $\text{put}(0) = \text{put}'(0) = 0$,

$$\begin{aligned}
\int_0^{K_l} K^\gamma \text{put}''(K)\,\mathrm{d}K &= K^\gamma \text{put}'(K)\Big|_0^{K_l} - \int_0^{K_l} \gamma K^{\gamma-1}\text{put}'(K)\,\mathrm{d}K \\
&= K_l^\gamma \text{put}'(K_l) - \left(\gamma K^{\gamma-1}\text{put}(K)\Big|_0^{K_l} - \int_0^{K_l} \gamma(\gamma-1)K^{\gamma-2}\text{put}(K)\,\mathrm{d}K\right) \\
&= K_l^\gamma \text{put}'(K_l) - \left(\gamma K_l^{\gamma-1}\text{put}(K_l) - \int_0^{K_l} \gamma(\gamma-1)K^{\gamma-2}\text{put}(K)\,\mathrm{d}K\right).
\end{aligned}$$

Plugging the expression back to the equation for $\mathbb{E}^*\left[R_m^\gamma \boldsymbol{I}(R_m \le q_l)\right]$ yields the second equation.

Finally, as

$$\mathbb{E}^*\left[R_m^\gamma \boldsymbol{I}(R_m \ge q_u)\right] = \frac{R_f}{S_0^\gamma}\int_{K_u}^{\infty} K^\gamma R_f \text{call}''(K)\,\mathrm{d}K,$$

following the same logic, we integrate the right-hand side integral by parts

$$\begin{aligned}
\int_{K_u}^{\infty} K^\gamma \text{call}''(K)\,\mathrm{d}K &= K^\gamma \text{call}'(K)\Big|_{K_u}^{\infty} - \int_{K_u}^{\infty} \gamma K^{\gamma-1}\text{call}'(K)\,\mathrm{d}K \\
&= -K_u^\gamma \text{call}'(K_u) - \left(\gamma K^{\gamma-1}\text{call}(K)\Big|_{K_u}^{\infty} - \int_{K_u}^{\infty} \gamma(\gamma-1)K^{\gamma-2}\text{call}(K)\,\mathrm{d}K\right) \\
&= -K_u^\gamma \text{call}'(K_u) + \left(\gamma K_u^{\gamma-1}\text{call}(K_l) + \int_{K_u}^{\infty} \gamma(\gamma-1)K^{\gamma-2}\text{call}(K)\,\mathrm{d}K\right)
\end{aligned}$$

where the second and third equations rely on the fact that $\text{call}'(\infty) = 0$ and $\text{call}(\infty) = 0$ respectively. Multiplying the last formula by R_f/S_0^γ leads to the third equation. □

B Calculating the Option-Implied Bounds

Here we provide further implementation details on calculating the option-implied bounds.

Filtering. We applied four criteria to filter the implied volatility data in our sample: 1) spot prices must be available from the CRSP database; 2) strike prices must be positive; 3) the OptionMetrics dispersion variable, a goodness-of-fit measure of OptionMetrics' multinomial tree algorithm, must be smaller than 0.05 and greater than zero; 4) for a given firm and time point, implied volatilities must be recorded at more than 10 different strike prices at the relevant maturity.

Interpolation and extrapolation. At time t, we denote by $\{\sigma_{it}(K_1,\tau),\ldots,\sigma_{it}(K_n,\tau)\}$

the Black-Scholes implied volatilities of firm i's stock at strike prices $K_1 \leq \cdots \leq K_n$, maturing at time $(t+\tau)$. These are observable volatility surface data from OptionMetrics. We linearly interpolate implied volatility observations for $K_1 < K < K_n$. For $K \leq K_1$, we let $\sigma_{it}(K,\tau) = \sigma_{it}(K_1,\tau)$; for $K \geq K_n$, we let $\sigma_{it}(K,\tau) = \sigma_{it}(K_n,\tau)$.

Risk-free rates. Risk-free rates are linearly interpolated from the OptionMetrics yield curve data.

The "clean" option prices. We construct option prices by applying the Black–Scholes formula for a given strike $K > 0$, maturity τ, implied volatility $\sigma_{it}(K,\tau)$, risk-free rate $r_t(\tau)$, and spot price S_{it}. These are European option prices assuming zero dividend yield. We compute these prices on a grid of 2000 steps within the interval $K/S_{it} \in [1/L,\, L]$, where $L = 3$ for one-, three-, and six-month horizons and $L = 5$ for the one-year horizon. We only consider out-of-the-money options. That is, when $K \leq S_{it}R_{f,t}$, we compute put option prices, where $R_{f,t} = \exp(r_t(\tau)\tau)$; when $K > S_{it}R_{f,t}$, we compute call option prices.

The risk-neutral marginals. Given put and call option prices on the grid of strikes, we numerically compute the following gradients to recover the risk-neutral marginals:

$$Q_{it}\left(\frac{K}{S_0}\right) = \begin{cases} R_{f,t}\mathrm{put}'_{it}(K), & K \leq R_{f,t}S_{it} \\ R_{f,t}\mathrm{call}'_{it}(K) + 1, & K > R_{f,t}S_{it} \end{cases}.$$

Only out-of-the-money option prices (derived from the corresponding implied volatilities) are used to compute the risk-neutral marginals. We fit an isotonic regression to the raw option-implied risk-neutral CDFs to guarantee their monotonicity. We then winsorize the fitted curve to ensure the CDFs are within [0, 1].

All procedures above are also applied to the S&P 500 index options.

We use Result 3 to compute the quantiles q_l and q_u, which involves both the risk-neutral marginals for individual stocks and those for the market index. When applying Result 5 to compute the numerators and denominators of our bounds, we use index option prices on the fine grid to numerically evaluate the integrals according to the midpoint rule.

C Constructing the Firm Characteristics

Firm characteristics used in the multiple regressions for crash probabilities are listed and described below. All variables are constructed using a merged CRSP-Compustat firm-month panel, unless otherwise noted.

Beta. The stock betas are estimated using daily return data within the windows of the last 12 months.

Relative size. The relative size is the difference between the market capitalization of a firm and the total market capitalization of the S&P 500 index in logarithmic terms.

Book to market ratio. The ratio is firms' book value of equities divided by their market capitalizations, calculated and updated at each fiscal quarter end.

Gross profitability. The numerator of this measure is the net revenue or the gross profit of a firm at the end of each fiscal quarter. If both of these quantities are missing, we use the summation of operating incomes and operating expenditures. The denominator is the market value of assets, calculated as a firm' market capitalization plus its book value of debts. Dividing the market value of total assets creates measures that are more sensitive to new firm-specific information (Campbell, Hilscher, and Szilagyi, 2008). Similarly, firm characteristics such *leverage*, *net income to asset*, and *cash to asset* ratios will also be scaled by the market value of assets throughout our analysis, as will be discussed later.

Momentum and reversals ($r_{(t-6)\to(t-1)}$, $r_{(t-12)\to(t-1)}$ and $r_{(t-1)\to t}$). These variables are lagged (net) equity returns of firms from month -6 to -1 and -12 to -1 (two momentum signals), as well as lagged one-month returns (reversals).

CHS-volatility. This measure is proposed in Chen, Hong, and Stein (2001) (CHS) for crash forecasting. The volatility is the rolling-window standard deviation of the excess of market returns ($R_i - R_m$), calculated based on daily return samples spanning the last six month.

Turnover. The stock turnover variable is defined as the monthly trading volume scaled by the number of shares outstanding. Following Chen, Hong, and Stein (2001), we use the average turnover over the lagged six-month data samples as our turnover characteristics. The trading volume on Nasdaq is adjusted according to the procedure detailed in Appendix B of Gao and Ritter (2010). Specifically, we divide Nasdaq volume by (1) 2.0 from January 1996 to January 2001; (2) 1.8 from February 2001to December 2001; (3) 1.6 from January 2002 to December 2003; (4) 1.0 after January 2004 to the end of our sample.

Sales growth. This variable is proposed for predicting industry-level stock crashes by Greenwood, Shleifer, and You (2019). To be considered, firms must have at least two consecutive years of revenue data. We calculate one-year sales growths based on the most recent observations of the changes in revenue.

Short interest. This characteristics is the fraction of shares held by institutional investors that have been sold short, as considered in Asquith, Pathak, and Ritter (2005); Daniel, Klos, and Rottke (2023). We divide the number of shares held short (available from Compustat) by the number of shares held by institutional investors (aggregated using Thomson-Reuters Institutional 13-F filings).

Leverage. We compute the leverage of a firm as its total liability (the book value of debts) divided by the market value of its total assets (calculated as a firm' market capitalization plus its book value of debts).

Net income to the market value of total asset. This variable is an additional measure of profitability based on the net income, proposed by Campbell, Hilscher, and Szilagyi (2008) in the study of bankruptcy forecast.

Cash to the market value of total asset. This characteristics is a liquidity measure with the numerator being cash and short-term investments, which is also incorporate in the econometric model of Campbell, Hilscher, and Szilagyi (2008) to forecast bankruptcy.

Log price per share. We also include the log share prices in the sample, winsorized from above at $15 per share (before taking logs) following Campbell, Hilscher, and Szilagyi (2008). This variable is mainly used to isolate the tendency of firms traded at low prices to crash.

To eliminate outliers, each of the fifteen characteristics described above are then winsorized within a 2.5 to 97.5 percentile interval. Table A1 tabulates the summary statistics of all the characteristics for our sample.

Table A1: Summary statistics of firm characteristics in our sample

char.	mean	sd	median	q25	q75	min	max
beta	1.031	0.500	0.985	0.691	1.296	0.126	2.521
relative size	−6.904	1.103	−7.007	−7.642	−6.272	−10.779	−2.618
book-to-market	0.468	0.330	0.377	0.234	0.615	0.055	1.545
gross profit.	0.159	0.097	0.145	0.092	0.204	0.014	0.487
$r_{(t-1)\to t}$	0.011	0.087	0.011	−0.039	0.060	−0.211	0.248
$r_{(t-6)\to(t-1)}$	0.066	0.219	0.063	−0.062	0.185	−0.452	0.729
$r_{(t-12)\to(t-1)}$	0.139	0.334	0.121	−0.064	0.309	−0.565	1.248
CHS-volatility	0.018	0.009	0.015	0.011	0.021	0.007	0.053
turnover	0.184	0.135	0.144	0.095	0.225	0.037	0.717
sales growth	0.084	0.201	0.059	−0.009	0.140	−0.334	0.918
short int.	0.046	0.067	0.026	0.015	0.047	0.003	0.426
leverage	0.442	0.221	0.400	0.269	0.599	0.107	0.913
net income/asset	0.025	0.024	0.026	0.015	0.038	−0.076	0.078
cash/asset	0.070	0.074	0.046	0.019	0.090	0.002	0.342
log price	2.679	0.137	2.708	2.708	2.708	1.733	2.708

D Additional Tables

Table A2: Relative bound widths: Fréchet–Hoeffding divided by Cauchy–Schwarz

This table reports summary statistics of the relative widths of bounds calculated according to Result 3 (based on the Fréchet–Hoeffding theorem, namely, the F-H bounds) and Equation 6 (based on the Cauchy–Schwarz inequality, namely, the C-S bounds). That is, the ratios reported here the ranges of the F-H bounds divided by the ranges of C-S bounds. We consider four different forecasting horizons and three crash sizes. For every month from January 1996 to December 2022, we compute the two types of bounds for each S&P 500 firm. The mean, standard deviation (sd), median, 25% and 75% sample quantile (q25 and q75), as well as the minimum and the maximum of the full firm-month panel are reported.

crash size	horizon	mean	sd	median	q25	q75	min	max
20%	1	0.291	0.170	0.269	0.160	0.411	0.000	0.800
20%	3	0.565	0.119	0.592	0.491	0.648	0.000	0.813
20%	6	0.659	0.071	0.662	0.623	0.706	0.000	0.811
20%	12	0.706	0.052	0.712	0.674	0.745	0.002	0.842
10%	1	0.544	0.107	0.565	0.487	0.618	0.000	0.848
10%	3	0.679	0.059	0.678	0.642	0.723	0.000	0.828
10%	6	0.727	0.043	0.733	0.698	0.761	0.000	0.812
10%	12	0.751	0.031	0.758	0.737	0.772	0.004	0.842
5%	1	0.615	0.083	0.630	0.578	0.668	0.000	0.849
5%	3	0.716	0.047	0.717	0.681	0.757	0.007	0.828
5%	6	0.751	0.033	0.761	0.735	0.775	0.098	0.812
5%	12	0.766	0.024	0.771	0.757	0.781	0.138	0.842

Table A3: Regression tests of the option-implied crash probability bounds: OLS with time fixed effects

This table reports the results from regressing the indicator function of realized equity returns being less than a threshold, q, on the option-implied physical probability bounds, $\mathbb{P}^L_{i,t}(\tau, q)$ and $\mathbb{P}^U_{i,t}(\tau, q)$, as well as the risk-neutral probabilities $\mathbb{P}^*_{i,t}(\tau, q)$. The data are monthly from January 1996 to December 2022. Firms under consideration are S&P 500 constituents. The return horizons, denoted by τ, are one month, three months, six months, and one year. Results in Panel A, B, C are from the linear regressions with time fixed effects,

$$\boldsymbol{I}(R_{i,t\to t+\tau} \leq q) = \alpha_t + \beta X_{it}(\tau, q) + \varepsilon_{i,t+\tau},$$

in which $q = 0.80, 0.90$ and 0.95, and X stands for $\mathbb{P}^L$ (the lower bounds), $\mathbb{P}^U$ (the upper bounds), or $\mathbb{P}^*$ (the risk-neutral probabilities). Values in parentheses are standard errors with two-way clustering following Thompson (2011). Values in square brackets are standard errors from block bootstrap using 2500 bootstrap samples following Martin and Wagner (2019). Projected R^2s are also reported.

	lower bound				upper bound				risk neutral			
horizon	1	3	6	12	1	3	6	12	1	3	6	12
Panel A: $q = 0.80$, down by over 20%												
β	0.93	1.04	1.13	1.11	0.62	0.68	0.74	0.72	0.73	0.81	0.89	0.87
	(0.09)	(0.07)	(0.06)	(0.06)	(0.06)	(0.04)	(0.04)	(0.04)	(0.07)	(0.05)	(0.05)	(0.05)
	[0.10]	[0.10]	[0.10]	[0.08]	[0.06]	[0.09]	[0.04]	[0.06]	[0.08]	[0.05]	[0.05]	[0.06]
R^2-proj	4.45%	4.66%	4.56%	4.11%	4.29%	4.46%	4.41%	4.08%	4.35%	4.54%	4.49%	4.10%
Panel B: $q = 0.90$, down by over 10%												
β	0.99	1.00	1.06	1.06	0.81	0.79	0.83	0.83	0.89	0.89	0.95	0.95
	(0.06)	(0.05)	(0.06)	(0.06)	(0.05)	(0.04)	(0.04)	(0.05)	(0.05)	(0.05)	(0.05)	(0.06)
	[0.07]	[0.08]	[0.06]	[0.06]	[0.05]	[0.05]	[0.06]	[0.07]	[0.06]	[0.05]	[0.08]	[0.09]
R^2-proj	4.02%	3.17%	3.18%	2.97%	3.96%	3.11%	3.14%	2.96%	3.98%	3.14%	3.17%	2.95%
Panel C: $q = 0.95$, down by over 5%												
β	0.87	0.86	0.97	0.97	0.77	0.76	0.85	0.86	0.83	0.82	0.93	0.93
	(0.05)	(0.05)	(0.07)	(0.07)	(0.04)	(0.05)	(0.06)	(0.06)	(0.05)	(0.05)	(0.06)	(0.07)
	[0.04]	[0.06]	[0.12]	[0.07]	[0.02]	[0.08]	[0.07]	[0.06]	[0.03]	[0.09]	[0.10]	[0.09]
R^2-proj	2.21%	1.62%	1.75%	1.84%	2.19%	1.60%	1.74%	1.85%	2.20%	1.61%	1.74%	1.84%

Table A4: Regression tests of the option-implied crash probability bounds: OLS with firm fixed effects

This table reports the results from regressing the indicator function of realized equity returns being less than a threshold, q, on the option-implied physical probability bounds, $\mathbb{P}^L_{i,t}(\tau, q)$ and $\mathbb{P}^U_{i,t}(\tau, q)$, as well as the risk-neutral probabilities $\mathbb{P}^*_{i,t}(\tau, q)$. The data are monthly from January 1996 to December 2022. Firms under consideration are S&P 500 constituents. The return horizons, denoted by τ, are one month, three months, six months, and one year. Results in Panels A, B and C are from the linear regressions with firm fixed effects,

$$\boldsymbol{I}(R_{i,t\to t+\tau} \leq q) = \alpha_i + \beta X_{it}(\tau, q) + \varepsilon_{i,t+\tau},$$

in which $q = 0.80, 0.90$ and 0.95, and X stands for $\mathbb{P}^L$ (the lower bounds), $\mathbb{P}^U$ (the upper bounds), or $\mathbb{P}^*$ (the risk-neutral probabilities). Values in parentheses are standard errors with two-way clustering following Thompson (2011). Values in square brackets are standard errors from block bootstrap using 2500 bootstrap samples following Martin and Wagner (2019). Projected R^2s are also reported.

	lower bound				upper bound				risk neutral			
horizon	1	3	6	12	1	3	6	12	1	3	6	12
					Panel A: $q = 0.80$, down by over 20%							
β	0.78	0.74	0.64	0.24	0.46	0.33	0.23	0.08	0.57	0.46	0.37	0.15
	(0.12)	(0.12)	(0.12)	(0.11)	(0.08)	(0.07)	(0.07)	(0.06)	(0.10)	(0.09)	(0.09)	(0.09)
	[0.12]	[0.15]	[0.16]	[0.26]	[0.09]	[0.11]	[0.06]	[0.08]	[0.09]	[0.05]	[0.10]	[0.10]
R^2-proj	2.91%	1.60%	0.86%	0.11%	2.83%	1.28%	0.53%	0.08%	2.89%	1.39%	0.67%	0.10%
					Panel B: $q = 0.90$, down by over 10%							
β	0.88	0.67	0.52	0.09	0.61	0.37	0.20	0.00	0.72	0.50	0.34	0.04
	(0.10)	(0.11)	(0.11)	(0.12)	(0.09)	(0.09)	(0.08)	(0.09)	(0.10)	(0.11)	(0.11)	(0.11)
	[0.10]	[0.16]	[0.18]	[0.17]	[0.11]	[0.19]	[0.09]	[0.10]	[0.11]	[0.14]	[0.17]	[0.19]
R^2-proj	2.48%	0.84%	0.39%	0.01%	2.60%	0.76%	0.22%	0.00%	2.60%	0.82%	0.32%	0.00%
					Panel C: $q = 0.95$, down by over 5%							
β	0.75	0.46	0.32	−0.11	0.58	0.25	0.07	−0.12	0.67	0.36	0.18	−0.15
	(0.09)	(0.10)	(0.11)	(0.13)	(0.10)	(0.12)	(0.11)	(0.11)	(0.10)	(0.12)	(0.13)	(0.14)
	[0.13]	[0.12]	[0.19]	[0.14]	[0.08]	[0.15]	[0.19]	[0.16]	[0.13]	[0.12]	[0.15]	[0.21]
R^2-proj	1.13%	0.25%	0.10%	0.01%	1.29%	0.19%	0.02%	0.06%	1.27%	0.23%	0.05%	0.04%

Table A5: Regression tests of the option-implied crash probability bounds: OLS with both time and firm fixed effects

This table reports the results from regressing the indicator function of realized equity returns being less than a threshold, q, on the option-implied physical probability bounds, $\mathbb{P}^L_{i,t}(\tau, q)$ and $\mathbb{P}^U_{i,t}(\tau, q)$, as well as the risk-neutral probabilities $\mathbb{P}^*_{i,t}(\tau, q)$. The data are monthly from January 1996 to December 2022. Firms under consideration are S&P 500 constituents. The return horizons, denoted by τ, are one month, three months, six months, and one year. Results in Panels A, B and C are from the linear regressions with both time and firm fixed effects,

$$\boldsymbol{I}(R_{i,t\to t+\tau} \le q) = \alpha_i + \lambda_t + \beta X_{it}(\tau, q) + \varepsilon_{i,t+\tau},$$

in which $q = 0.80, 0.90$ and 0.95, and X stands for $\mathbb{P}^L$ (the lower bounds), $\mathbb{P}^U$ (the upper bounds), or $\mathbb{P}^*$ (the risk-neutral probabilities). Values in parentheses are standard errors with two-way clustering following Thompson (2011). Values in square brackets are standard errors from block bootstrap using 2500 bootstrap samples following Martin and Wagner (2019). Projected R^2s are also reported.

	lower bound				upper bound				risk neutral			
horizon	1	3	6	12	1	3	6	12	1	3	6	12
					Panel A: $q = 0.80$, down by over 20%							
β	0.73	0.59	0.38	0.04	0.49	0.38	0.24	0.05	0.58	0.46	0.30	0.05
	(0.09)	(0.07)	(0.06)	(0.06)	(0.06)	(0.04)	(0.04)	(0.04)	(0.07)	(0.05)	(0.05)	(0.05)
	[0.10]	[0.07]	[0.08]	[0.07]	[0.07]	[0.07]	[0.04]	[0.04]	[0.09]	[0.06]	[0.06]	[0.06]
R^2-proj	1.76%	0.74%	0.25%	0.00%	1.68%	0.68%	0.23%	0.01%	1.71%	0.70%	0.24%	0.01%
					Panel B: $q = 0.90$, down by over 10%							
β	0.65	0.35	0.18	−0.04	0.53	0.27	0.15	0.00	0.58	0.31	0.17	−0.01
	(0.05)	(0.05)	(0.05)	(0.06)	(0.04)	(0.04)	(0.04)	(0.04)	(0.05)	(0.04)	(0.05)	(0.05)
	[0.08]	[0.05]	[0.05]	[0.06]	[0.06]	[0.04]	[0.04]	[0.02]	[0.04]	[0.06]	[0.06]	[0.06]
R^2-proj	0.90%	0.18%	0.04%	0.00%	0.88%	0.18%	0.05%	0.00%	0.89%	0.18%	0.05%	0.00%
					Panel C: $q = 0.95$, down by over 5%							
β	0.43	0.19	0.03	−0.16	0.39	0.17	0.05	−0.10	0.41	0.19	0.05	−0.13
	(0.04)	(0.04)	(0.05)	(0.06)	(0.03)	(0.04)	(0.04)	(0.05)	(0.04)	(0.04)	(0.05)	(0.06)
	[0.04]	[0.08]	[0.06]	[0.08]	[0.03]	[0.04]	[0.09]	[0.06]	[0.03]	[0.04]	[0.08]	[0.05]
R^2-proj	0.30%	0.04%	0.00%	0.03%	0.30%	0.04%	0.00%	0.01%	0.30%	0.04%	0.00%	0.02%

Table A6: Regression tests of the option-implied crash probability bounds: adjusted regressions for 20% crash in one quarter

This table reports the results from the following regressions:

$$\boldsymbol{I}(R_{i,t\to t+3} \leq 0.80) = \beta \cdot X_{it}(\tau, 0.80) + \lambda \cdot \text{controls}_{it} + \varepsilon_{i,t+3},$$

in which X stands for $\mathbb{P}^L$ (the lower bounds), $\mathbb{P}^*$ (the risk-neutral probability), or both. The controls are fifteen firm characteristics from the literature. All independent variables are transformed to have a unit standard deviation. Regression coefficients are reported as percentage points, and their two-way clustered standard errors are included in the parentheses. The first five columns are simple OLS estimates, and the sixth column reports estimates with time fixed effects, with a projected (within) R^2 replacing the standard ones. Asterisks indicate coefficients whose t-statistics exceed four in magnitude.

	$\boldsymbol{I}(R_{t\to t+3} \leq 0.8)$					
	(1)	(2)	(3)	(4)	(5)	(6)
$\mathbb{P}^L[R_{t\to t+3} \leq 0.8]$		5.75*	4.23*		10.79	3.62*
		(0.51)	(0.75)		(2.83)	(0.33)
$\mathbb{P}^*[R_{t\to t+3} \leq 0.8]$				2.66	−6.53	
				(0.81)	(2.92)	
beta	1.14		0.34	0.73	0.11	0.91
	(0.31)		(0.34)	(0.35)	(0.32)	(0.26)
relative size	−0.31		−0.25	−0.33	−0.10	0.01
	(0.27)		(0.26)	(0.26)	(0.26)	(0.17)
book-to-market	−0.30		−0.34	−0.32	−0.37	0.13
	(0.21)		(0.21)	(0.21)	(0.21)	(0.17)
gross profit.	−0.05		−0.05	−0.06	−0.02	0.11
	(0.19)		(0.18)	(0.19)	(0.18)	(0.15)
$r_{(t-1)\to t}$	−0.48		−0.27	−0.31	−0.36	−0.09
	(0.38)		(0.38)	(0.38)	(0.37)	(0.20)
$r_{(t-6)\to(t-1)}$	−0.78		−0.63	−0.66	−0.70	−0.50
	(0.47)		(0.48)	(0.48)	(0.45)	(0.28)
$r_{(t-12)\to(t-1)}$	−0.06		−0.15	−0.08	−0.24	−0.69
	(0.48)		(0.48)	(0.48)	(0.47)	(0.32)
CHS-volatility	4.13*		1.39	2.35	1.52	1.09
	(0.53)		(0.68)	(0.72)	(0.66)	(0.37)
turnover	0.59		0.17	0.33	0.18	0.72
	(0.55)		(0.52)	(0.52)	(0.51)	(0.26)
sales growth	0.55		0.49	0.55	0.42	0.25
	(0.20)		(0.20)	(0.20)	(0.20)	(0.12)
short int.	1.03*		0.94*	1.02*	0.83*	0.69*
	(0.19)		(0.18)	(0.19)	(0.18)	(0.14)
leverage	−0.19		−0.05	−0.14	0.07	−0.06
	(0.23)		(0.23)	(0.23)	(0.22)	(0.20)
net income/asset	−0.48		−0.36	−0.47	−0.22	−0.33
	(0.24)		(0.24)	(0.24)	(0.23)	(0.15)
cash/asset	−0.25		−0.42	−0.34	−0.46	−0.15
	(0.17)		(0.17)	(0.18)	(0.17)	(0.13)
log price	0.37		0.80	0.57	0.96	0.48
	(0.22)		(0.22)	(0.21)	(0.24)	(0.17)
intercept	−0.12	−0.01	−0.18	−0.16	−0.20*	
	(0.05)	(0.01)	(0.05)	(0.05)	(0.05)	
R^2/R^2-proj.	5.06%	5.17%	5.70%	5.36%	5.96%	5.24%

Table A7: Regression tests of the option-implied crash probability bounds: adjusted regressions for 20% crash in one year

This table reports the results from the following regressions:

$$\boldsymbol{I}(R_{i,t\to t+12} \leq 0.80) = \beta \cdot X_{it}(\tau, 0.80) + \lambda \cdot \text{controls}_{it} + \varepsilon_{i,t+12},$$

in which X stands for $\mathbb{P}^L$ (the lower bounds), $\mathbb{P}^*$ (the risk-neutral probability), or both. The controls are fifteen firm characteristics from the literature. All independent variables are transformed to have a unit standard deviation. Regression coefficients are reported as percentage points, and their two-way clustered standard errors are included in the parentheses. The first five columns are simple OLS estimates, and the sixth column reports estimates with time fixed effects, with a projected (within) R^2 replacing the standard ones. Asterisks indicate coefficients whose t-statistics exceed four in magnitude.

	$\boldsymbol{I}(R_{t\to t+12} \leq 0.8)$					
	(1)	(2)	(3)	(4)	(5)	(6)
$\mathbb{P}^L[R_{t\to t+12} \leq 0.8]$		6.96*	5.28*		9.17*	4.37*
		(0.54)	(0.73)		(2.09)	(0.42)
$\mathbb{P}^*[R_{t\to t+12} \leq 0.8]$				2.55	−4.56	
				(0.95)	(2.22)	
beta	0.94		−0.26	0.54	−0.43	1.17
	(0.42)		(0.43)	(0.48)	(0.42)	(0.41)
relative size	−0.89		−0.32	−0.74	−0.17	0.32
	(0.44)		(0.44)	(0.46)	(0.44)	(0.34)
book-to-market	−1.35		−1.38	−1.37	−1.37	0.02
	(0.41)		(0.40)	(0.41)	(0.40)	(0.32)
gross profit.	−0.66		−0.67	−0.68	−0.64	−0.03
	(0.38)		(0.37)	(0.37)	(0.37)	(0.32)
$r_{(t-1)\to t}$	−0.38		−0.18	−0.23	−0.29	−0.45
	(0.55)		(0.54)	(0.55)	(0.52)	(0.25)
$r_{(t-6)\to(t-1)}$	−1.47		−1.39	−1.40	−1.46	−0.73
	(0.67)		(0.65)	(0.67)	(0.62)	(0.34)
$r_{(t-12)\to(t-1)}$	1.17		0.92	1.11	0.84	0.33
	(0.64)		(0.63)	(0.64)	(0.61)	(0.49)
CHS-volatility	5.32*		2.20	3.64	2.92	2.18
	(0.77)		(0.90)	(0.93)	(0.88)	(0.56)
turnover	0.83		0.48	0.63	0.58	0.65
	(0.81)		(0.80)	(0.79)	(0.77)	(0.42)
sales growth	2.00*		1.86*	1.99*	1.78*	0.93
	(0.34)		(0.34)	(0.34)	(0.34)	(0.23)
short int.	2.42*		2.28*	2.40*	2.22*	2.04*
	(0.41)		(0.40)	(0.41)	(0.40)	(0.32)
leverage	−0.44		−0.11	−0.36	−0.01	−0.23
	(0.42)		(0.41)	(0.43)	(0.41)	(0.36)
net income/asset	−0.91		−0.71	−0.91	−0.57	−0.38
	(0.39)		(0.38)	(0.39)	(0.37)	(0.30)
cash/asset	−0.62		−0.89	−0.72	−0.91	−0.40
	(0.32)		(0.31)	(0.33)	(0.31)	(0.25)
log price	1.41		1.96*	1.58*	2.07*	1.18
	(0.36)		(0.37)	(0.36)	(0.37)	(0.31)
intercept	−0.28	0.02	−0.37*	−0.33*	−0.35*	
	(0.08)	(0.01)	(0.08)	(0.08)	(0.08)	
R^2/R^2-proj.	4.59%	3.76%	5.16%	4.74%	5.31%	4.99%

Table A8: Area under the curve (AUC) statistics for out-of-sample forecasting: option-implied lower bounds vs. characteristic-based statistical models

This table reports AUCs (in percentage points) of forecasting whether a stock's return will crash over 20%, using the option-implied lower bounds (OIB-LB), as well as statistical procedures based on stock characteristics and risk-neutral crash probability (RN). Stocks of firms belonging to the S&P 500 index are considered. The data are monthly from January 1996 to December 2022. The return horizons are one month, three month, six months, and one year. The training samples start at January 1996 and end at December 2006, December 2011, or December 2016. The remaining data serve as our testing sample. The two statistical procedures under consideration are linear and logistic regressions, with variables selected by the LASSO (OLS-Lasso and Logistic-Lasso). The LASSO tuning parameters for sparsity control are selected to maximize in-sample AUCs according to five-fold cross validations. AUCs (%) are then reported for the testing samples.

	AUC statistics (%)			
maturity	1	3	6	12
Panel A: Training Sample 1996-2006				
OIB-LB	85.89	72.00	67.95	63.65
OLS-Lasso	80.63	70.05	66.38	61.62
Logistic-Lasso	80.92	70.23	66.04	61.57
OLS-Lasso w. RN	85.80	70.88	66.81	61.79
Logistic-Lasso w. RN	84.10	71.15	66.61	61.69
Panel B: Training Sample 1996-2011				
OIB-LB	84.99	69.04	67.46	65.09
OLS-Lasso	77.04	68.83	66.63	62.66
Logistic-Lasso	77.10	68.81	66.62	62.38
OLS-Lasso w. RN	84.88	68.98	66.95	62.89
Logistic-Lasso w. RN	84.93	68.79	66.80	62.61
Panel C: Training Sample 1996-2016				
OIB-LB	83.92	63.41	63.57	62.19
OLS-Lasso	71.58	61.98	60.93	57.11
Logistic-Lasso	72.09	62.36	60.08	56.94
OLS-Lasso w. RN	83.70	62.00	61.17	57.92
Logistic-Lasso w. RN	83.40	61.40	61.31	57.50